Idaho National Engineering and Environmental Laboratory

INEEL/EXT-99-00678

September 2000

Long Term Corrosion/Degradation Test First Year Results

R. E. Mizia
M. K. Adler Flitton
C. W. Bishop
L. L. Torres
R. D. Rogers
S. C. Wilkins

BECHTEL BWXT IDAHO, LLC

INEEL/EXT-99-00678

Long Term Corrosion/Degradation Test First Year Results

R. E. Mizia
M. K. Adler Flitton
C. W. Bishop
L. L. Torres
R. D. Rogers
S. C. Wilkins

Published September 2000

Idaho National Engineering and Environmental Laboratory

Idaho Falls, Idaho 83415

Prepared for the
U.S. Department of Energy

Under DOE Idaho Operations Office
Contract DE-AC07-99ID13727

ABSTRACT

The Subsurface Disposal Area (SDA) of the Radioactive Waste Management Complex located at the Idaho National Engineering and Environmental Laboratory contains neutron-activated metals from non-fuel, nuclear reactor core components.

The Long-Term Corrosion/Degradation Program test is designed to obtain site-specific corrosion rates to support efforts to more accurately estimate the transfer of activated elements to the environment. This report describes the test program and documents the corrosion rates of non-radioactive metals, representing the prominent activated material buried at the SDA, after one year of underground exposure to corrosion conditions.

The prominent neutron activated metals are Type 304L and 316L stainless steels, Inconel 718, Beryllium S200F, Aluminum 6061, and Zircaloy-4. Additionally, carbon steel (the material presently used in the disposal liners of the 55-ton scrap cask and other disposal containers) and Ferralium 255 (the proposed material for the high integrity disposal containers) are also included in the test program.

In the first year results, no measurable corrosion was reported for types 304L and 316L stainless steel, Inconel 718, and Zircaloy-4. The corrosion rate for Ferralium 255 ranged from no measurable corrosion to a maximum rate of 0.0005 mils per year (MPY) (1.27×10^{-8} m/year). These rates are two orders of magnitude lower than those specified in the performance assessment for the SDA. The maximum measured corrosion rate for the aluminum was 0.0028 MPY (7.1×10^{-8} m/year).

The corrosion rates for carbon steel and beryllium were much higher, up to 0.1102 MPY (2.8×10^{-6} m/year), with surface corrosion products and pit initiation being evident. The corrosion rate for beryllium should be investigated further, as beryllium contains significant quantities of tritium after exposure to neutron irradiation.

ACKNOWLEDGMENTS

The first-year results for the Long Term Corrosion/Degradation Test culminates an effort of more than three years. The support of Infrastructure necessary to successfully pursue the objectives of the project has been vast, and besides the authors of this document, many have contributed to the success of the project. Foremost has been the programmatic support from John Logan and others who have continued to champion funding for the project's continuation. An integrated team of engineers and scientists participated in both project and laboratory support. Some of the supporting expertise came from Peter Nagata, Brad Norby, Larry Hull, Craig Dickie, Cathy Pfeifer, Colleen Shelton-Davies, Evan Hales, Phil Anderson, Jim Turpin, Bob Mahoney, and Bill Colson. Operation support included planners, schedulers, Craft personnel, Safety (Leon Hunsaker and Jim O'Brien), and Industrial Hygienists (Grayson Downs, Craig Davis, and Kirk Chadwick). Paramount has been the challenge to obtain high quality results with impeccable technical credibility while maintaining a safe work environment. As the project continues into successive phases and as new challenges arise, appreciation is extended to all those who have made significant contributions.

CONTENTS

FIGURES

TABLES

ACRONYMS

ASTM	American Society for Testing and Materials
ATR	Advanced Test Reactor
CA	Coupon Array
Ci	curie
DOE	Department of Energy
EBTF	Engineered Barriers Test Facility
Inconel	Trade Mark of Inco Alloys International
INEEL	Idaho National Engineering and Environmental Laboratory
INTEC	Idaho Nuclear Technology & Engineering Center
LTCD	long term corrosion/degradation
MPY	mils per year
NAG	nutrient agar with glucose
NIST	National Institute for Standards Testing
PRG	phenol red agar with glucose
RWMC	Radioactive Waste Management Complex
SDA	Subsurface Disposal Area
SRB	sulfate reducing bacteria

Long Term Corrosion/Degradation Test First Year Results

1. INTRODUCTION

The Radioactive Waste Management Complex (RWMC) Subsurface Disposal Area (SDA) at the Idaho National Engineering and Environmental Laboratory (INEEL) has been a major disposal site for solid radioactive waste since the early 1950s. The SDA contains low-level waste, transuranic waste, hazardous waste, and mixed waste. Since 1970, incoming waste generally has been segregated according to waste type before disposal, and transuranic waste has been stored instead of being place in disposal. A large portion of the radioactive content of the waste disposed at the SDA is represented by neutron-irradiated metals, consisting mostly of reactor core structural components (subassemblies, cladding, and other non-fuel reactor core components) composed of stainless steel, nickel-based alloys (such as Inconel 718), and other metals.

The large amount of neutron-irradiated metal buried at the SDA represents an environmental concern. The irradiation produces long lived (C-14, Ni-59, Nb-94, Tc-99) and short lived (Co-60, Ni-63) radioactive isotopes (10 CFR 61). (In addition, a possible short-term release rate component is the tritium that is formed under neutron irradiation in the Advanced Test Reactor (ATR) reflectors composed of beryllium.) The radioactive isotopes are produced inside the crystalline structure of the metal, and most of the isotopes are assumed to be released to the environment only through metallic corrosion (Rood and Adler Flitton, 1997). Thus, for these isotopes, the calculated release rate is driven by the assumed corrosion rate.

The Department of Energy (DOE) Order 435.1a (DOE 1999), "Radioactive Waste Management" (formerly DOE Order 5820.2A) requires a radiological composite analysis and a performance assessment of existing and proposed DOE low-level waste facilities. As of this writing (September 2000), an updated SDA performance assessment is currently being drafted to replace the current one. For the current SDA performance assessment (Maheras, et al. 1994), corrosion times for a variety of reactor components were obtained using the IMPACTS methodology (Oztunali and Roles 1986). Corrosion times in the SDA performance assessment are based on corrosion rates of 4 mils per year (MPY) (1.02×10^{-4} m/year) for carbon steel and 0.3 MPY (7.62×10^{-6} m/year) for stainless steel, respectively. The corrosion rates for the stainless steel are rates from the IMPACTS study for austenitic stainless steels (Types 304 and 316) in natural waters and seawater.

The rates at which the irradiated metals buried at the SDA actually corrode might be different than the "textbook" corrosion rates assumed in the SDA performance assessment. For example, a recent study reviewed corrosion rates for low carbon steels, Types 304 and 316 stainless steels, and Inconel 600, 601, and 718 alloys in SDA-type soils (Nagata and Banaee 1996). That study estimated that the corrosion rate for the stainless steels and the Inconel 718 in environments with geochemistry similar to that of the SDA soils was 0.00047 MPY (1.2×10^{-8} m/year), which is about two orders of magnitude lower than the corrosion rate assumed in the SDA performance assessment for stainless steel.

Site-specific underground corrosion rate data do not currently exist for metals exposed to SDA soils. Textbook corrosion rates are typically derived from testing in water or in soils that are wetter and less alkaline than SDA soils. In order to accurately calculate the release rates for irradiated metals buried at the SDA, site-specific corrosion rate data are needed.

The Long-Term Corrosion/Degradation (LTCD) Test Project described in this report will determine the SDA site-specific corrosion rates of the neutron-activated metals buried at the SDA. The

project began in 1997 and will continue, as funding permits, as long as 32 years or until enough data have been collected to satisfy the requirements of the radiological composite analysis, the performance assessment, and the environmental baseline risk assessment for the SDA. The project is using non-radioactive coupons of representative alloys to determine the relevant corrosion rates, by placing the coupons in soil taken from the same location as the soil used as backfill to cover the waste buried at the SDA (that is, soil from "Spreading Area B"). The materials included in the test are Types 304 and 316 stainless steels, Inconel 718, Beryllium S200F, Aluminum 6061, and Zircaloy-4 (the list recommended by Rood and Adler Flitton, 1997), broadly representing the irradiated metals buried at the SDA. In addition, carbon steel (the material presently used in the disposal liners of the 55-ton scrap cask and other disposal containers) and Ferralium 255 (a proposed material for construction of high integrity disposal containers) are included as part of the test.

This report describes the LTCD Test Project, documents the placement of the coupons, presents the results of the first year coupon retrieval and evaluation, discusses related studies conducted to support the project, draws tentative conclusions, and makes recommendations for the future conduct of the testing.

1.1 Objective

The LTCD test is designed to determine the corrosion rates of metallic materials buried at the SDA. The corrosion rate data are needed to provide a more accurate estimate of the radiological release rates. Of interest are the metallic materials used to fabricate nuclear reactor components that were exposed to high neutron fluxes in a reactor environment, such that they became activated with long-lived radioactive isotopes. After disposal, corrosion processes can cause these radioactive isotopes to be released to the environment. The current SDA performance assessment (Maheras et al. 1994) postulates that the largest release factor during the corrosion process will be from C-14, which would be released from the surface of buried metals.

The LTCD test is designed to provide an underground disposal environment similar to that in which the neutron-activated metals are buried at the SDA. The objective is to obtain site-specific corrosion rates that will support accurate estimates of the transfer of radioactive isotopes to the environment (release rate). Corrosion and degradation rates will be established for non-radioactive metals, representing the prominent activated material buried at the SDA, including low-carbon steel, Types 304L and 316L stainless steel, Inconel 718, Beryllium S200F, Aluminum 6061, Zircaloy-4, and Ferralium 255. The project's use of non-radioactive metal coupons assumes that activation does not affect corrosion characteristics or mechanisms.

Environmental conditions existing or potentially existing at the SDA affect the corrosion rates of metals buried there. Underground corrosion rates are directly related to soil characteristics. SDA backfill soil (from Spreading Area B) will be characterized chemically, physically, hydraulically, and microbiologically during the course of the LTCD test project.

1.2 Document Organization

This report documents all work to date related to the LTCD project. Section 2 describes the test location, materials, and coupon emplacement process. Section 3 describes the results of the first year coupon retrieval and evaluation, including measurement results, corrosion rates, and uncertainties. Section 4 presents a discussion of related studies, including a soil moisture study, a soil microbiology study, and comparisons with studies at other sites. Section 6 presents conclusions and recommendations. References are listed in Section 7. Appendix A provides the material certification documentation for the test materials. Appendix B describes the techniques used in the soil microbiology study. Appendix C provides data related to the pitting of the carbon steel and beryllium.

2. DIRECT-BURIED CORROSION COUPON TEST METHODOLOGY

2.1 Test Location

The LTCD test location is near the SDA. The corrosion coupons are exposed to the same soil and environmental conditions as the activated metals buried in the SDA, but the test location is not directly in the SDA. The LTCD tests are being conducted at a specially constructed test site adjacent to the Engineered Barriers Test Facility (EBTF), located north of the RWMC SDA, as shown in Figure 1.

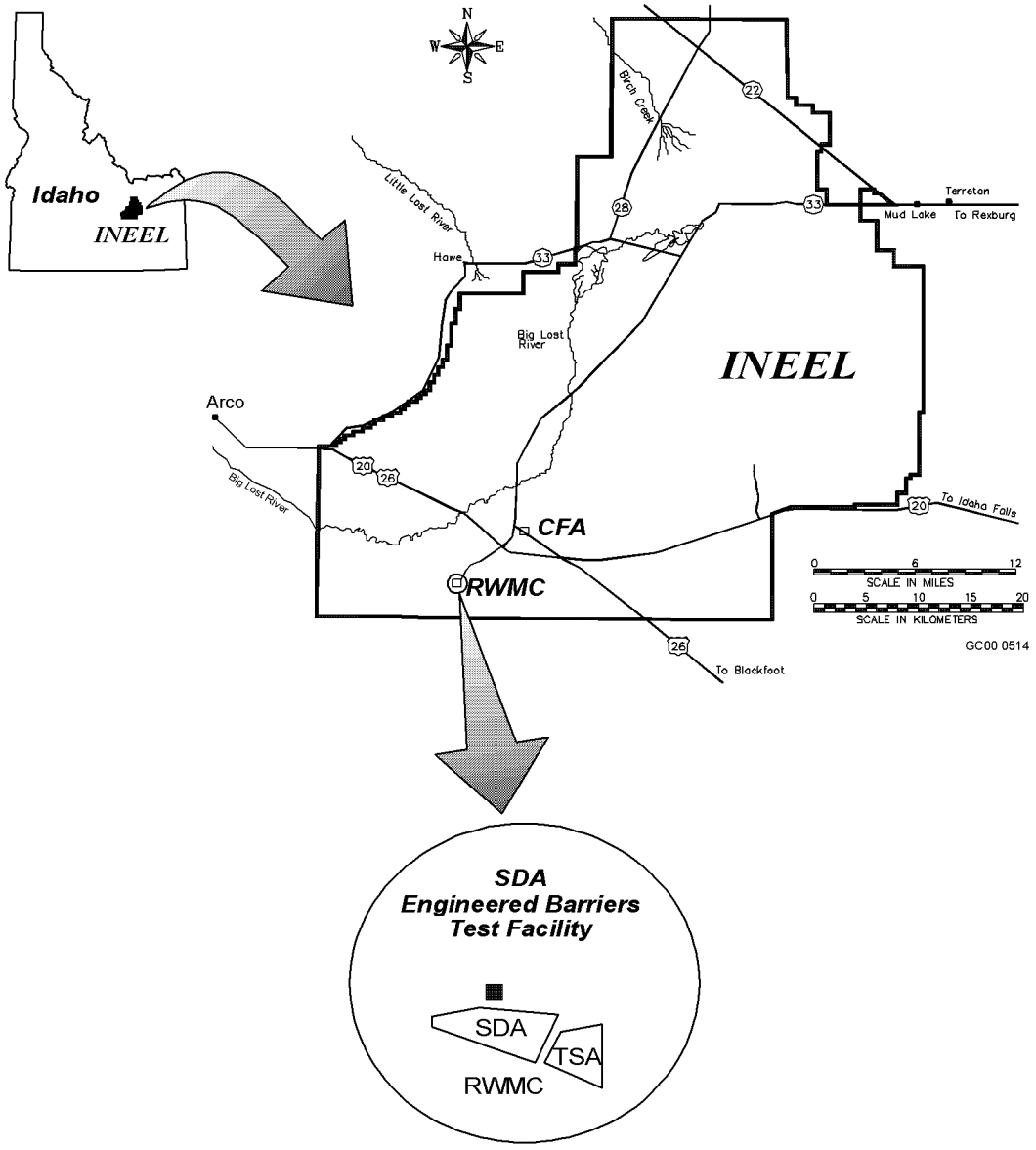

Figure 1. Site of the RWMC SDA at the INEEL.

Direct burial in the SDA was not feasible for the following reasons:

- The SDA has limited access because of radiological concerns
- Limited space is available in the SDA for coupon emplacement
- The logistics of moving and cleaning samples with possible radiological contamination are too complex
- The final soil cover might be placed on the SDA before retrieval of the last coupons.

The EBTF was constructed earlier, for testing of the hydrological performance of prospective engineered barriers for use at the SDA. The EBTF, shown in Figure 2, was expanded on the east side to form the Engineered Barriers Extension (EBE), where the LTCD tests are being conducted (see Figure 3). The EBE consists of a mound of backfill (soil) from Spreading Area B. The mound has sloping sides and a flat top, providing a useable working area of 85 ft by 88 ft. For brevity and convenience, this report refers to the LTCD test location (the EBE) as the Berm.

Four specific locations at the Berm were selected for placement of the coupons, to accommodate burial of two sets of 36 coupons at two depths at each location. (Each set of 36 coupons, after assembly, is referred to here as a coupon array.) The four locations are shown in Figure 4.

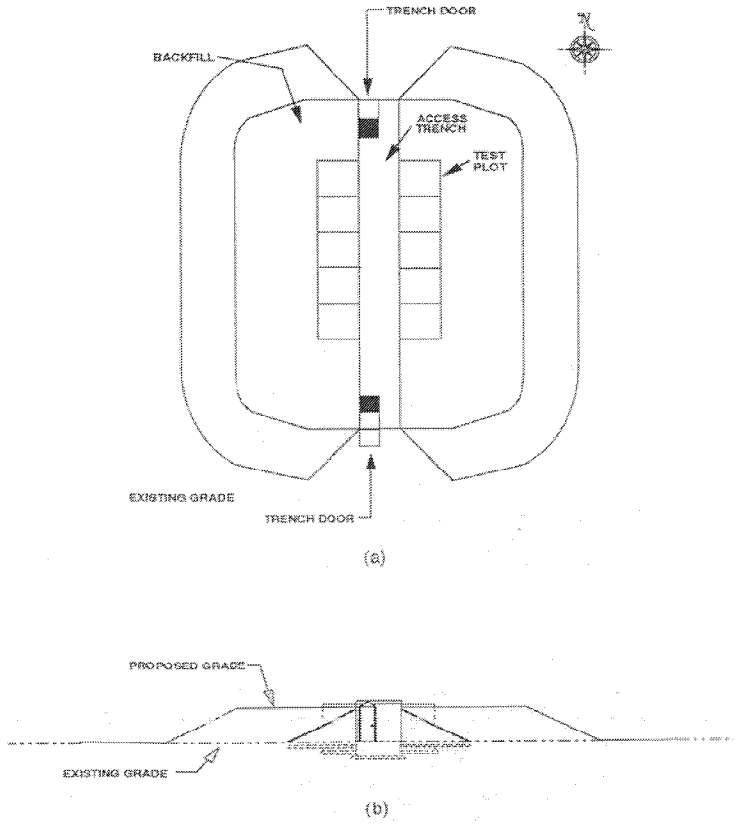

Figure 2. Engineered Barriers Test Facility.

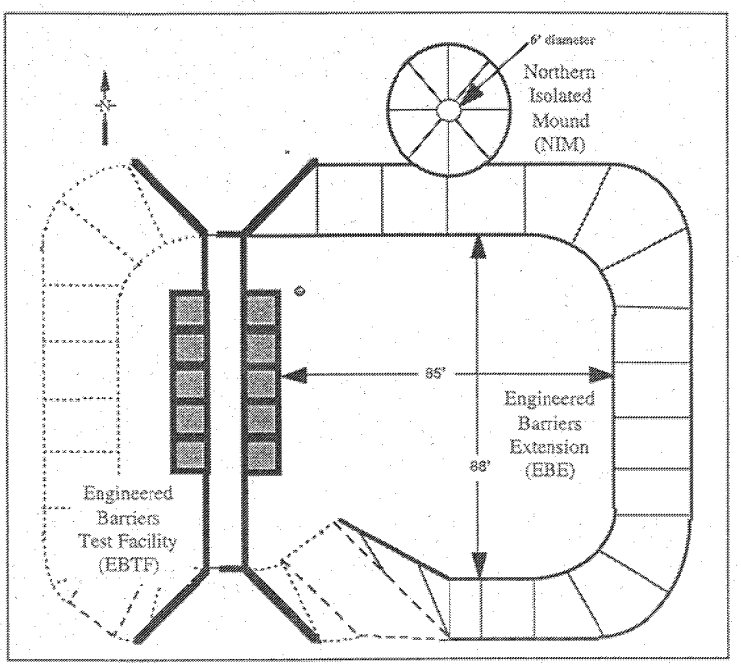

Figure 3. Engineered Barriers Extension (the Berm).

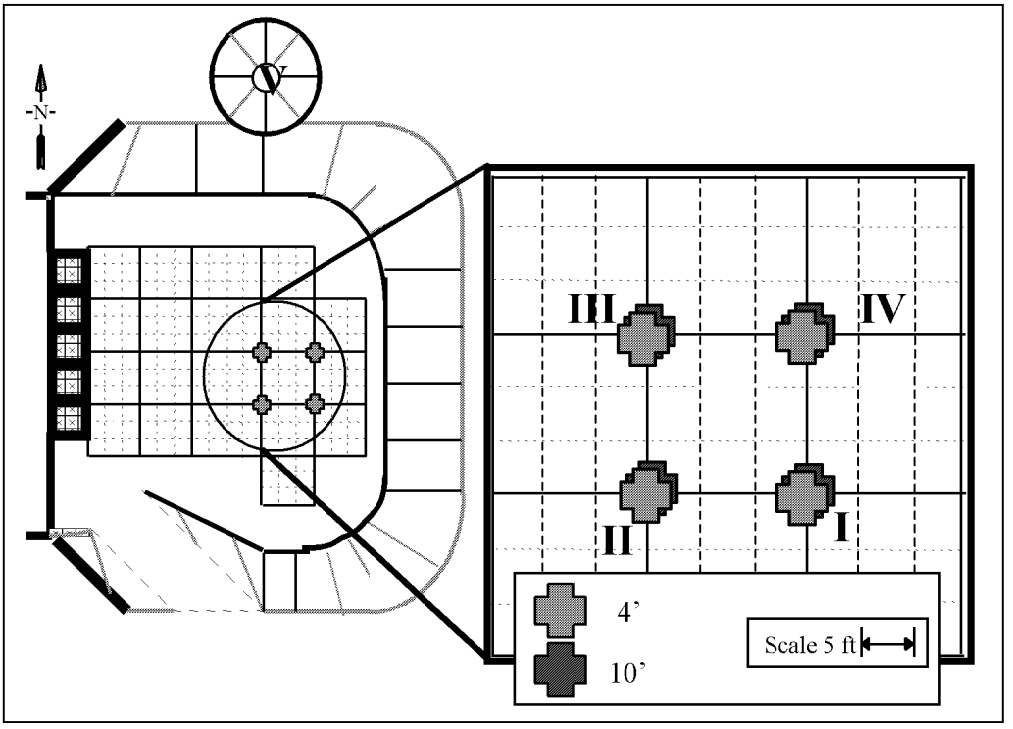

Figure 4. Coupon array locations at the Berm.

The configuration shown in Figure 4 arranges the coupon placement locations in a grid with spacing of 15 ft center to center. This arrangement separates the coupon arrays by a minimum of 10 ft, so that recovery of any one coupon array will not disturb the soil and corresponding soil characteristics (soil gas, soil moisture, and soil chemistry) in other test locations. (Different coupon arrays will be in place for different time periods.) The coupon array locations were placed at least 20 ft from the edge of the berm to minimize any edge effects. A setback of 10 ft from the existing EBTF structure ensures a buffer zone. A minimum of 65 ft (west to east) is required to accommodate two rows of coupon arrays. With two rows, a minimum of 85 ft (north to south) would accommodate as many as eight coupon array locations.

Representative soil samples were collected from the Berm at the locations where the coupon arrays were to be installed, and at other locations, as shown in Figure 5. To collect these samples, each of the four coupon array locations were core drilled (CA-CH1, 2, 3, and 4). These core holes served as the center for the six-ft diameter holes used to install the coupon arrays. Two locations reserved as spare coupon array locations not yet used (CA-CH5 and 6) were likewise core drilled and sampled, along with two other locations (IB-CH7 and AP-CH8). Ten soil samples were collected from each hole at one-ft intervals, from the surface to 10-ft below surface.

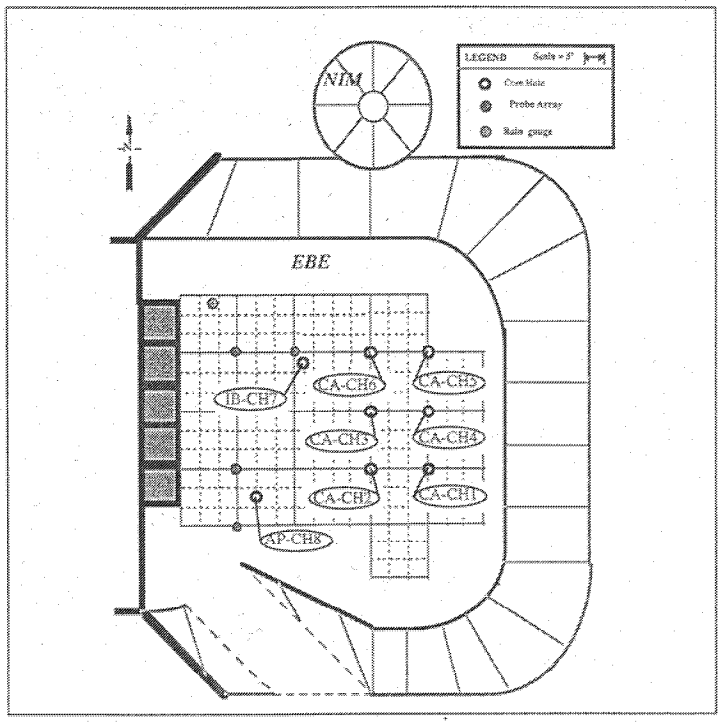

Figure 5. Core holes for soil samples.

2.2 Test Coupons And Materials

A study by Rood and Adler Flitton (1997) determined that Types 304/304L and 316/316L stainless steels, Inconel 718, Beryllium S200F, Aluminum 6061, and Zircaloy-4 were appropriate materials to be included in the LTCD Test Project. The decision was based on the amounts and types of material present at the SDA, and on the conclusion that these alloys produce activation products after exposure in a neutron flux. Carbon steel was added because of the large, underground corrosion database available for this material and because it is used for the disposal liners of the 55-ton scrap cask and for various other disposal containers buried at the SDA. Ferralium 255 (a duplex stainless steel) was also added to the list,

as it was the prospective material for high integrity disposal containers that might be used in the future for disposal of some wastes.

The corrosion coupons are 3 X 3 X 1/8 in. (Figures 6 and 7) with a 0.56-in.-diameter hole in the center. Before burial, the coupons were stamped with a unique identification number, and they were measured, cleaned, and weighed in accordance with the requirements of American Society for Testing and Materials (ASTM) Method G1, and the weights and surface area measurements recorded. The coupon surface finish is 120 grit, except for the beryllium coupons, which have a 125 RMS finish. Each coupon was individually photographed on a background sheet that contains the coupon number, material, surface area, and weight (Figure 6 is an example). All coupon data were recorded in controlled lab notebooks (LN-875, 876, 877, 879, 887, 888, 890, 948) that are stored by the Materials Development and Technology group at the Idaho Nuclear Technology & Engineering Center (INTEC) Facility.

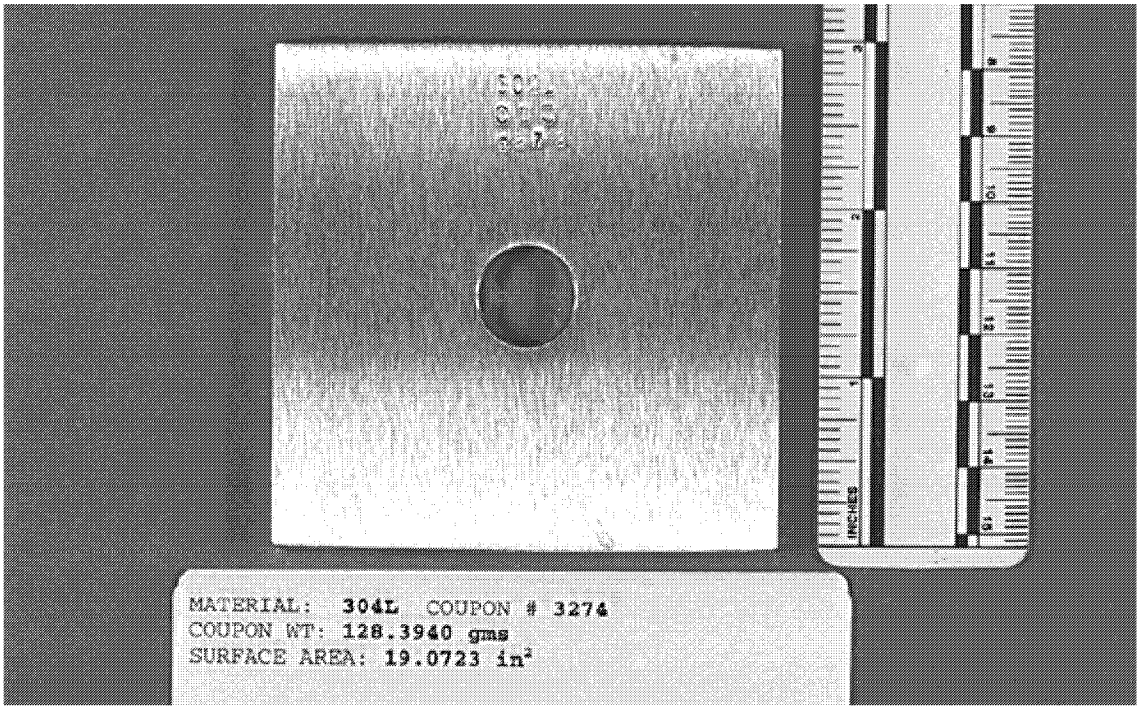

Figure 6. Typical corrosion coupon, 304L stainless steel.

The coupons were assembled onto coupon arrays constructed of polypropylene rods with Teflon tubing as spacers (Figure 7), with a 6-in. minimum separation between coupons. Polypropylene and Teflon were selected because these inert materials are expected not to chemically or electrically interfere with the corrosion of the coupons. Each coupon array consists of six polypropylene rods (of three different lengths), with the coupons and Teflon spacers installed on the rods as shown in Figure 8. Each end of the polypropylene rod has engraved Teflon identification markers and is secured with a threaded nylon nut. Each coupon array consists of four test coupons of each of the following metals: low-carbon steel, Types 304L and 316L stainless steel, welded Type 316L stainless steel, Inconel 718, Beryllium S200F, Aluminum 6061, Zircaloy-4, and Ferralium 255, for a total of 36 coupons. In the assembly of the coupon arrays, the locations of coupons of various material types were randomly selected. The certified material test reports for the coupons are provided in Appendix A.

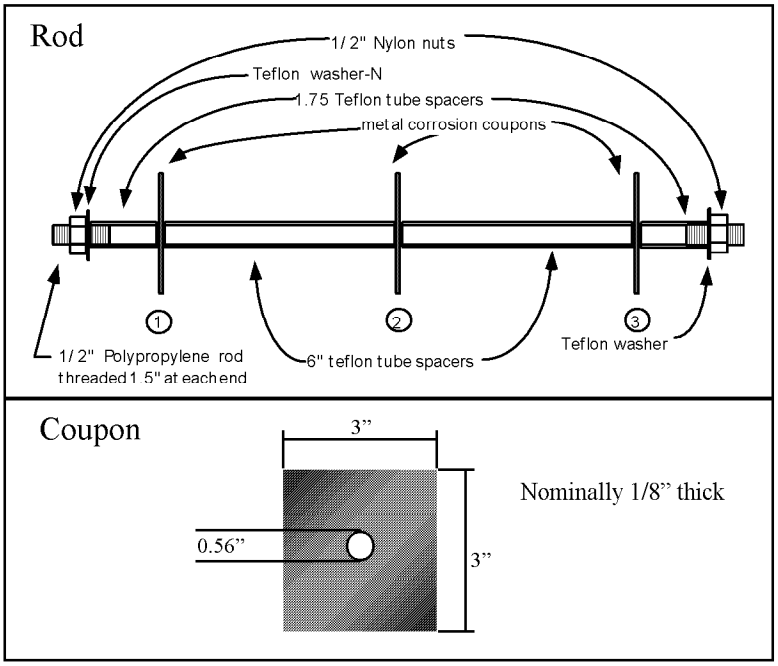

Figure 7. Corrosion coupon assembly details.

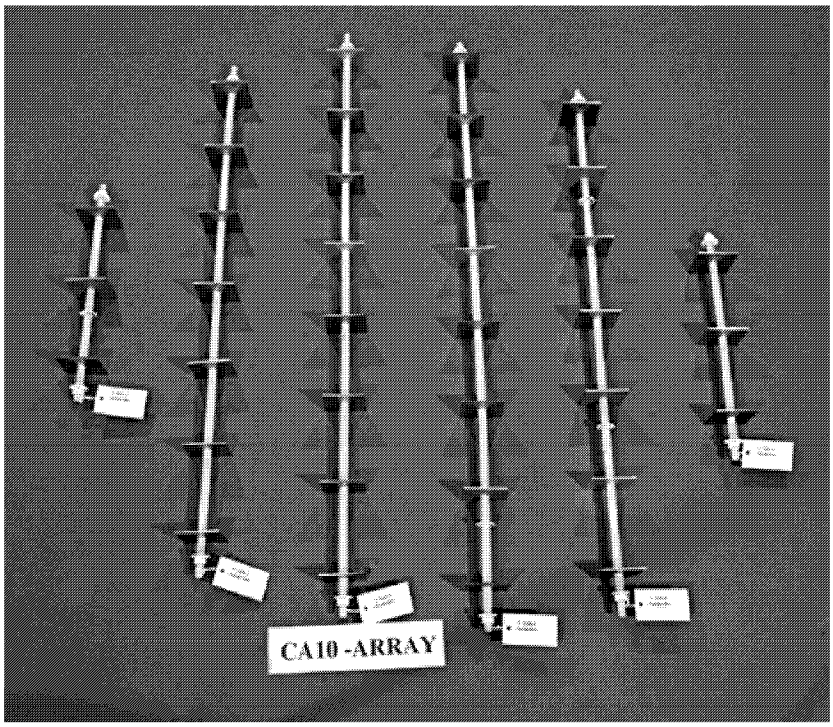

Figure 8. Coupon array.

Twelve sets of 36 coupons were prepared and slated for testing. (Most of these have already been buried, as described later in this report.) In addition, two complete sets are stored at the INTEC. One of these is maintained as a reserve set, for possible burial at a later date, and the other was archived for comparison with the timed test.

Since identification numbers on the individual coupons might degrade during the test, a secondary method of identification is also employed. Each coupon has a specific coordinate in the coupon array and is assigned a test identification number based on this placement. An example of the coupon array/corrosion coupon nomenclature is: CA01-1-1. The first four digits refer to the coupon array number, the next number refers to the rod number in the array, and the last number refers to the coupon position on that rod. Figure 9 illustrates this nomenclature system. After the corrosion coupons were placed on the coupon arrays, photographs were taken of each array for baseline documentation. A map was made showing the location of each coupon as originally placed on the coupon array.

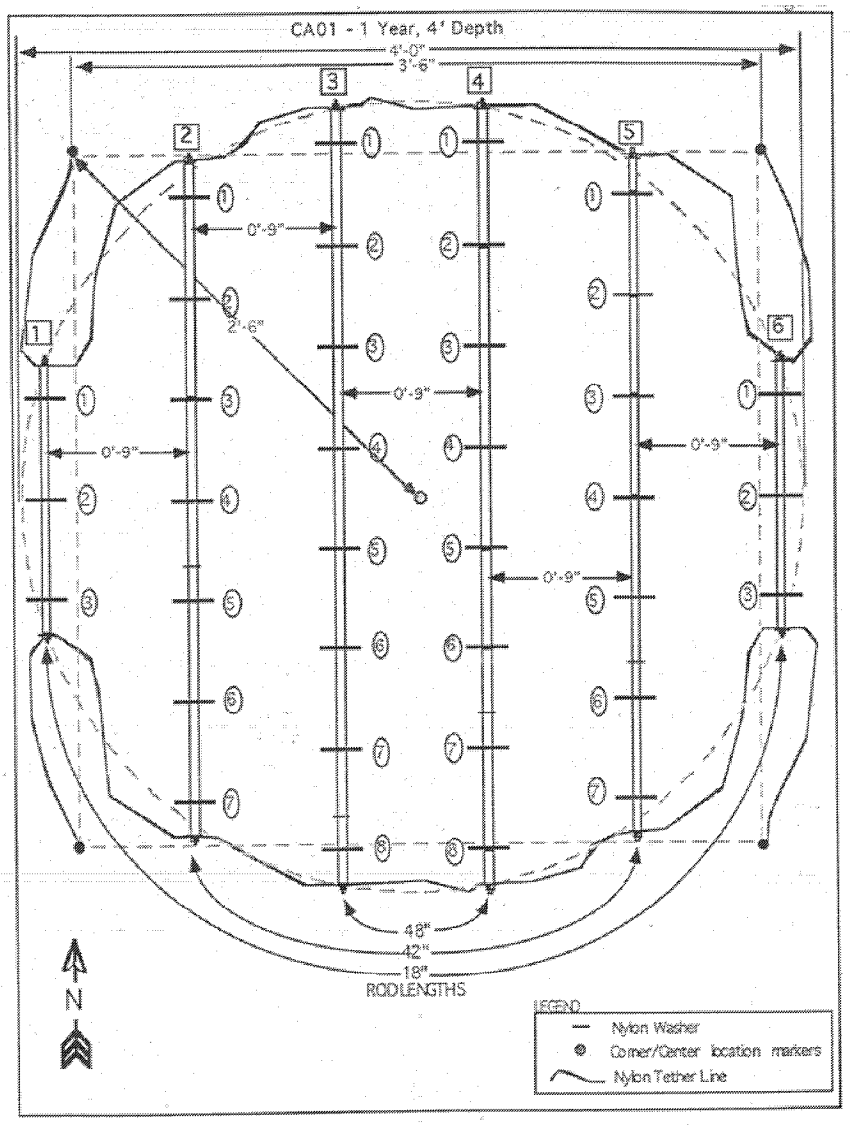

Figure 9. Numbering system for coupons installed in a coupon array.

2.3 Coupon Array Emplacement

In the autumn of 1997, coupon arrays were buried at depths of 4 ft and 10 ft at each of the four locations identified in Figure 4, for a total of eight coupon arrays. The 4- and 10-ft corrosion array burial depths were chosen to represent the activated core components that are buried from 4 ft to a maximum of 20 ft below the surface. The 4-ft depth provides a high level of exposure to changing environmental conditions, while the 10-ft depth more closely represents actual buried waste storage conditions. At each location, a hole was drilled using a drill rig equipped with a 6-ft-diameter auger (see Figure 10). Coupon arrays, each consisting of six polypropylene rod assemblies, were placed in the holes, with nine inches separation between the rods. A typical coupon array placed in a hole is shown in Figure 11.

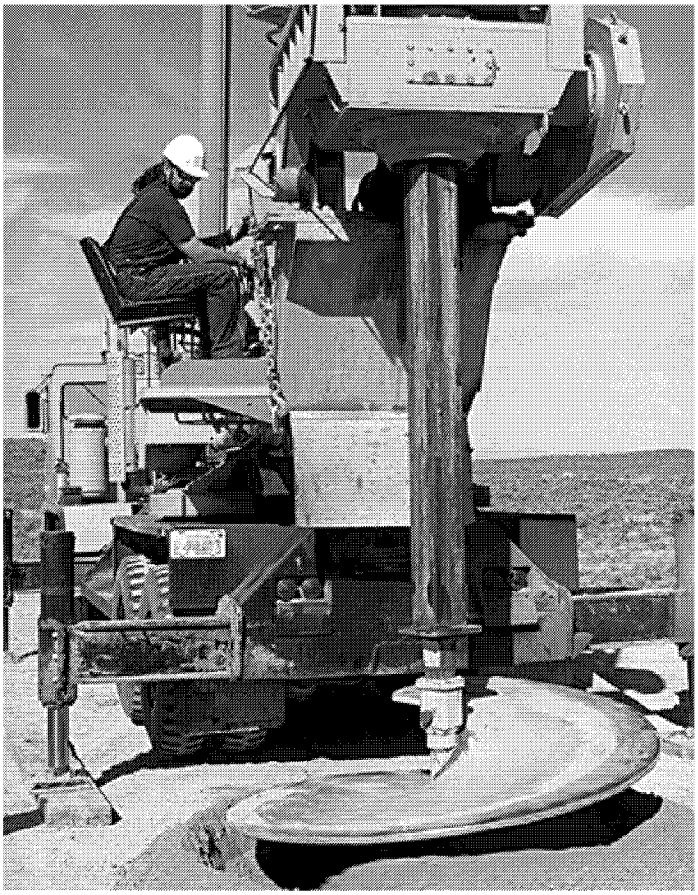

Figure 10. Drill rig with 6-ft-diameter auger.

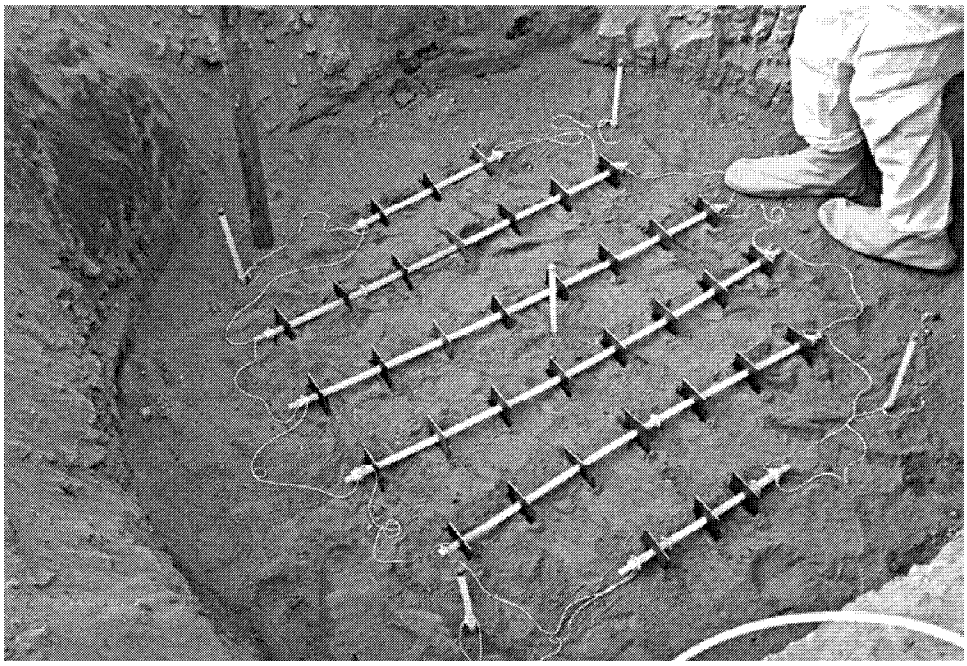

Figure 11. Coupon array in test hole.

By way of comparison, previous corrosion testing of stainless steels performed at various sites by the National Institute of Standards and Technology (NIST) (Gerhold et al. 1976; Gerhold et al. 1981) placed the coupons in shallow trenches (about 3-ft deep and 2-ft wide). The classic underground corrosion test by Romanoff (1957) placed the corrosion coupons at depths where underground piping would commonly be buried at the location. The depths ranged from 18 in. to 6 ft. The underground corrosion test at the DOE Hanford Site was designed to allow deep burial of up to 30 feet (Bunnel et al. 1994). Review articles by Escalante (1987, 1995) recommend a burial depth of approximately one meter.

The first three holes were drilled and the corresponding six coupon arrays were installed on October 20, 21, and 22, 1997. The fourth hole was drilled and the corresponding two coupon arrays were installed November 3, 1997.

Following burial of each coupon array at the 10-ft level, the 6-ft diameter hole was back-filled in 8-in. lifts with Spreading Area B soil and manually compacted to approximately the 4-ft level, at which the second coupon array was placed. The hole was back-filled to the surface using 8-in. lifts with manual compaction.

The coupon installation and retrieval schedule is shown in Table 1. The original schedule provided for corrosion measurements to be performed after one, two, four, eight, sixteen, and thirty-two years. Reductions in funding for the program have impacted that schedule, such that the current schedule calls for corrosion measurements after one, three, and four years, with out-years yet to have programmatic funding identified.

Table 1. Coupon installation and retrieval schedule.

Depth below berm surface		Date Installed	Date Recovered	Location (Figure 4)
4 feet	10 feet			
CA01		Oct. 22, 1997	Oct. 23, 1998	I
	CA02	Oct. 21, 1997	Nov. 3-5, 1998	
CA03		Oct. 22, 1997	October 2000 [a]	II
	CA04	Oct. 21, 1997	October 2000 [a]	
CA05		Nov. 3, 1997	October 2001 [a]	III
	CA06	Nov. 3, 1997	October 2001 [a]	
CA07		Oct. 22, 1997	October 2005 [a]	IV
	CA08	Oct. 22, 1997	October 2005 [a]	
CA09		Nov. 10, 1998	October 2014 [a]	I
	CA10	Nov. 11, 1998	October 2014 [a]	
CA11		October 2000 [a]	October 2032 [a]	II [b]
	CA12	October 2000 [a]	October 2032 [a]	
CA13		To be determined	To be determined	V [b]

[a] Planned dates (as of June 2000).
[b] Planned locations (as of June 2000).

3. FIRST YEAR CORROSION RESULTS

3.1 Coupon Array Removal

After coupon arrays CA01 and CA02 had been exposed to corrosion conditions for approximately one year, they were removed for corrosion measurement. The coupons were recovered by reopening the hole with a backhoe, manually, and with the 6-ft auger drill. The backhoe dug to 3 ft, then the hole was manually opened from the 3-ft level to the 4-ft level, and CA01 was removed. The drill then dug to approximately 8 ft, with the remaining soil excavated manually. (Experience proved that it would have been better not to use the backhoe, since it caused the top edges of the hole to be unstable.) The coupons were extracted carefully from the hole, with care not to loosen the soil around them. The excavated coupons were transported in containers to the appropriate laboratory, disassembled, and the corrosion products sampled. A typical transport container is shown in Figure 12. The coupon array after transport to the laboratory is shown in Figure 13.

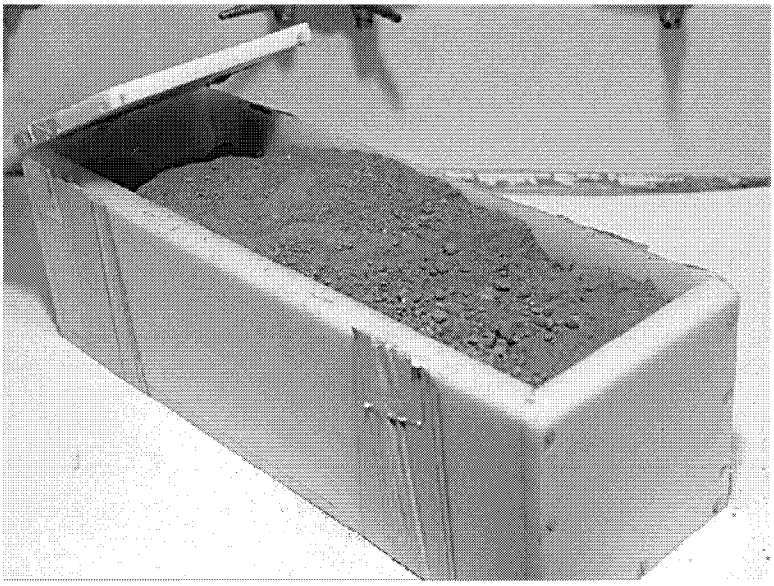

Figure 12. Single rod transport container.

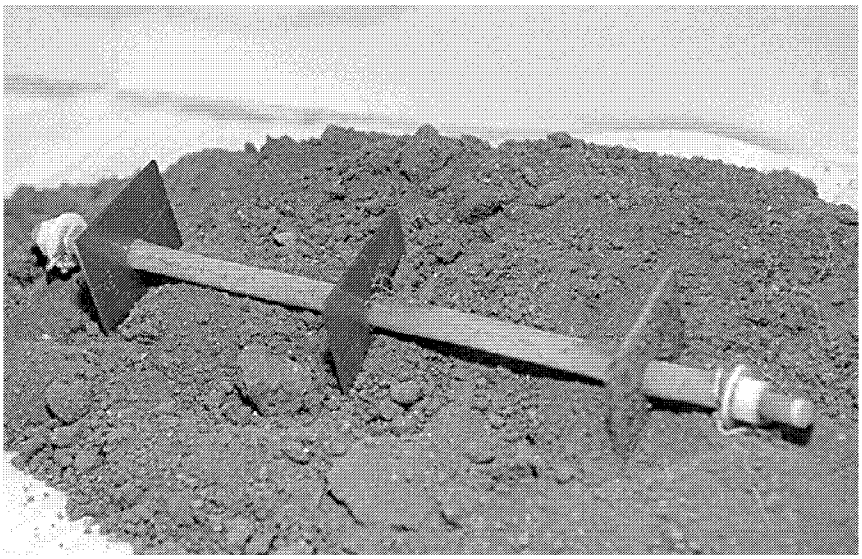

Figure 13. Rod from coupon array after removal from transport container.

3.2 Coupon Cleaning

The coupon cleaning process is designed to remove all corrosion products from the coupons. The weight of the coupon after corrosion and cleaning is compared to the original weight, and the difference represents the loss of metal to corrosion.

All one-year corrosion coupons were cleaned with a washing/brushing process, per the requirements of ASTM G1 6.2.1, using de-ionized water and a nonmetallic soft bristle brush. The Ferralium 255, 304L and 316L stainless steels, Inconel 718, and Zircaloy-4 coupons required no further cleaning. The aluminum, beryllium, and carbon steel coupons were chemically cleaned according to ASTM G-1 (in addition to the wash/brush process). The beryllium coupons were cleaned to the ASTM magnesium cleaning standard C.5.2. This technique was recommended by the materials vendor (Brush-Wellman). The carbon steel coupons were cleaned with ASTM chemical cleaning procedure C.3.5. The aluminum coupons were chemically cleaned per ASTM designation C.1.1.

All cleaning activities for all alloys, along with weights taken after each cleaning cycle, were recorded in the lab notebooks. To ensure that all deposits were removed and that the coupons were clean, cleaning curves were calculated for the coupons in accordance with ASTM Method G1.

3.3 Weight Loss Measurement Method

After the one-year corrosion coupons were cleaned, they were weighed on the Mettler 163 balance. The weight was subtracted from the original weight of the coupon (before exposure), as recorded in the laboratory notebooks, to calculate the weight loss due to corrosion, and the corresponding corrosion rate was calculated. The coupons were also examined with a stereo microscope for localized corrosion (pitting, etc). All samples, including the coupons and metallographic specimens, are archived and stored with the Materials Development Group.

Weight loss was measured in grams, and the corrosion rate was calculated in mils per year (MPY). The typical corrosion rate calculation is as follows:

$$\text{Corrosion Rate (MPY)} = \frac{10 \times \text{weight loss (g)} \times 39.37}{\text{Density (g/cm}^3\text{)} \times \text{Area (cm}^2\text{)} \times \text{Time (year)}}$$

The results are presented in Section 3.5.

3.4 Weight-Loss Measurement Uncertainties

The corrosion rate is calculated from a coupon weight loss measurement, so it is important that uncertainties associated with the weight loss measurement be accounted for. This is especially true for the stainless steels and other metals whose corrosion rates are anticipated to be very low. Measurement uncertainties for the LTCD Tests are of three types:

- Statistical errors for the Mettler 163 balance used to weigh the coupons
- Possible loss of base metal (in addition to corrosion material) to the wash/brush process
- Possible loss of base metal (in addition to corrosion material) to the chemical treatment.

The laboratory balance measurement uncertainty was investigated for the range of corrosion coupon weights, that is, at 50, 100, and 150 grams. (Coupon weights range from a low of about 37 g for the beryllium coupons to a high of about 146 g for the Inconel 718 coupons.) Balance uncertainties (2σ, 95% confidence level) were found to be ± 0.4 mg for the 50- and 100-gram balance ranges and ± 0.8 mg for the 150-gram balance range. The results are presented in Table 2.

Table 2. Balance variability from reference weight measurements.

Reference Weight (gm)	Number of Measurements	Average Measurement Value (gm)	Standard Deviation (gm)
50	80	50.004	0.0002
100	80	100.0010	0.0002
150	80	150.0016	0.0004

A study was also performed to measure the corrosion coupon weight loss due to the wash/brush cleaning. A series of coupon cleaning tests were conducted to collect statistically reliable weight-loss data for typical coupon cleaning processes (Wilkins et al. 1998).

The testing consisted of cleaning uncorroded 304L/316L stainless steels and Inconel 718 coupons with the wash/brush process and recording the subsequent weight change. The results are shown in Table 3. These results apply only to the compositions tested (304L/316L stainless steels and Inconel 718). Available funds did not allow for similar tests on the other coupon compositions.

Table 3. Weight loss of uncorroded coupons during the wash/brush process.

Material (cleaning solution)	Test Run	Average Weight Change (gm)	Standard Deviation (gm)	Overall Avg. Weight Change (gm)	Overall Standard Deviation (gm)
304L	1	0.0001	0.0002	-0.0001	0.0004
	2	-0.0005	0.0003		
	3	-0.0001	0.0004		
	4	-0.0003	0.0001		
	5	-0.0001	0.0003		
316L	1	-0.0000	0.0003	-0.0001	0.0005
	2	-0.0007	0.0002		
	3	-0.0002	0.0003		
	4	-0.0003	0.0004		
	5	-0.0000	0.0004		
Inconel 718	1	-0.0004	0.0002	-0.0002	0.0003
	2	-0.0003	0.0003		
	3	0.0000	0.0002		
	4	-0.0003	0.0002		
	5	-0.0002	0.0002		

The data from Tables 2 and 3 are combined in Table 4, which describes the combination of these uncertainties to give the minimum detectable corrosion rates. A sufficient number of coupons and cleaning cycles were used to provide statistically significant uncertainties for the processes. The combined cleaning/weighing uncertainties found for the wash/brush cleaning process, at a 95% confidence level, were ± 0.89 mg for 304L stainless steel, ± 0.98 mg for 316L stainless steel, and ± 0.92 mg for Inconel 718. Again, these combined results apply only to the three materials that were tested with the wash/brush process. The uncertainties determined for the weighing process (Table 2) can be applied to all coupon compositions, however.

Together, the studies show a small uncertainty. For most of the coupons, the measurement of very low weight losses from one year exposure fall within the balance variability and cleaning weight-loss measurements. For the results reported in Section 3.5, whenever the measured weight loss is less than either the balance variability or the combined uncertainty (as applicable), the corrosion rate is listed as "No reportable corrosion."

Table 4. Minimum detectable corrosion rates – wash/brush cleaning process.

Material	Ave. Wt. Change (gm)	Combined 95% Uncertainty (gm)	Minimum Detectable Corrosion Rate (one year)	
			mm/year	mils/year
304L	-0.0001	0.00089	8.3×10^{-6}	3.3×10^{-4}
316L	-0.0001?	0.00098	1.0×10^{-5}	3.9×10^{-4}
Inconel -718	-0.0002	0.00092	8.3×10^{-6}	3.3×10^{-4}

One-year corrosion coupons composed of beryllium, aluminum, and carbon steel were subjected to a chemical cleaning process (in addition to the wash/brush process). To address concerns about uncertainties introduced by the chemical cleaning process, a blank (uncorroded) specimen of the same material was run through the chemical cleaning process along with the corroded test specimens. The blank specimen was one of the reserved archived samples and thus from the same heat (lot) as the corroded test coupons. The weight losses measured after cleaning the blank coupons are listed in Table 5. The weight losses reported in Table 5 were subtracted from the weight losses of the corresponding corroded coupons to arrive at the weight loss due to corrosion, as reported in Section 3.5.

Table 5. Cleaning blanks weight losses.

Beryllium S200F	36.5781-36.5770 = 0.0011 g
Aluminum 6061 T6	44.1394-44.1377 = 0.0017 g
CS 1018	130.0959-130.0833 = 0.0661 g

3.5 Weight Loss Measurement Results

In all, 72 one-year coupons were recovered, cleaned, and weighed. The weight losses for the individual coupons, along with the corresponding corrosion rates (calculated as explained in Section 3.3), are presented in Tables 6 and 7 for coupons buried at 4-ft and 10-ft depths, respectively. A notation of "No reportable corrosion" indicates that no weight loss was measured or that the measured weight loss was less than the uncertainties described in Section 3.4 (uncertainties due to variability in the balance

Table 6. Corrosion results after 8788 hours (about one year) for coupons buried at 4 ft.

Coupon location	Composition	Identifier	Weight loss (g)	Corrosion rate (MPY)
CAO1-2-1	Aluminum	3478	0.0011	0.0013
CAO1-3-2	Aluminum	3479	0.0004	0.0005
CAO1-4-1	Aluminum	3480	0.0024	0.0028
CAO1-5-5	Aluminum	3481	0.0000	No Reportable Corrosion
CAO1-2-5	Beryllium	S / N - 1	0.0150	0.025
CAO1-3-8	Beryllium	S / N - 2	0.0589	0.099
CAO1-4-7	Beryllium	S / N - 3	0.0480	0.081
CAO1-5-6	Beryllium	S / N - 4	0.0662	0.111
CAO1-1-1	Carbon Steel	3322	0.3193	0.13
CAO1-2-2	Carbon Steel	3323	0.3501	0.14
CAO1-3-5	Carbon Steel	3324	0.3012	0.12
CAO1-4-4	Carbon Steel	3325	0.2780	0.11
CAO1-1-3	Ferralium 255	W3732	0.0001[a]	No Reportable Corrosion
CAO1-3-1	Ferralium 255	W3733	Weight Gain 0.0002[a]	No Reportable Corrosion
CAO1-4-8	Ferralium 255	W3734	0.0012	0.0005
CAO1-6-2	Ferralium 255	W3735	0.0010	0.0004
CAO1-2-3	Inconel 718	3424	0.0001[a]	No Reportable Corrosion
CAO1-3-4	Inconel 718	3425	Weight Gain 0.0005[a]	No Reportable Corrosion
CAO1-4-6	Inconel 718	3426	0.0000[a]	No Reportable Corrosion
CAO1-5-4	Inconel 718	3427	0.0000[a]	No Reportable Corrosion
CAO1-2-4	304L	3268	0.0006[a]	No Reportable Corrosion
CAO1-3-6	304L	3269	Weight Gain 0.0001[a]	No Reportable Corrosion
CAO1-5-3	304L	3270	0.0001[a]	No Reportable Corrosion
CAO1-5-1	304L	3271	Weight Gain 0.0003[a]	No Reportable Corrosion
CAO1-1-2	316L	3364	0.0005[a]	No Reportable Corrosion
CAO1-4-3	316L	3365	0.0004[a]	No Reportable Corrosion
CAO1-5-2	316L	3366	0.0004[a]	No Reportable Corrosion
CAO1-6-1	316L	3367	0.0008[a]	No Reportable Corrosion
CAO1-2-6	316L Welded	W3672	Weight Gain 0.0007[a]	No Reportable Corrosion
CAO1-3-7	316L Welded	W3673	Weight Gain 0.0004[a]	No Reportable Corrosion
CAO1-4-2	316L Welded	W3674	Weight Gain 0.0005[a]	No Reportable Corrosion
CAO1-5-7	316L Welded	W3675	Weight Gain 0.0003[a]	No Reportable Corrosion
CAO1-2-7	Zircaloy-4	3792	Weight Gain 0.0010	No Reportable Corrosion
CAO1-3-3	Zircaloy-4	3793	Weight Gain 0.0013	No Reportable Corrosion
CAO1-4-5	Zircaloy-4	3794	Weight Gain 0.0007	No Reportable Corrosion
CAO1-6-3	Zircaloy-4	3795	Weight Gain 0.0009	No Reportable Corrosion

a. weight loss or gain (if any) is within the tolerance of the Mettler AE 163 Balance

Table 7. Corrosion results after 9116 hours (about one year) for coupons buried at 10 ft.

Coupon location	Composition	Identifier	Weight Loss (g)	Corrosion Rate (MPY)
CAO2-1-2	Aluminum	3482	0.0000*	No Reportable Corrosion
CAO2-1-3	Aluminum	3483	0.0011*	0.0013
CAO2-3-7	Aluminum	3484	0.0005*	No Reportable Corrosion
CAO2-4-1	Aluminum	3485	0.0006*	No Reportable Corrosion
CAO2-2-5	Beryllium	S / N - 5	0.0932	0.152
CAO2-4-4	Beryllium	S / N - 10	0.1084	0.176
CAO2-4-7	Beryllium	S / N - 11	0.1138	0.185
CAO2-5-7	Beryllium	S / N - 12	0.1239	0.202
CAO2-2-3	Carbon Steel	3326	0.6996	0.27
CAO2-3-2	Carbon Steel	3327	0.5961	0.23
CAO2-3-6	Carbon Steel	3328	0.5661	0.22
CAO2-4-3	Carbon Steel	3329	0.7095	0.28
CAO2-2-2	Ferralium 255	W3736	0.0007*	No Reportable Corrosion
CAO2-3-4	Ferralium 255	W3737	0.0010	0.0004
CAO2-4-2	Ferralium 255	W3738	0.0012	0.0005
CAO2-5-4	Ferralium 255	W3739	0.0011	0.0004
CAO2-2-7	Inconel 718	3428	Weight gain 0.0004*	No Reportable Corrosion
CAO2-4-6	Inconel 718	3429	0.0006*	No Reportable Corrosion
CAO2-5-2	Inconel 718	3430	0.0000*	No Reportable Corrosion
CAO2-5-3	Inconel 718	3431	0.0000*	No Reportable Corrosion
CAO2-2-4	304L	3272	0.0004*	No Reportable Corrosion
CAO2-3-1	304L	3273	0.0004*	No Reportable Corrosion
CAO2-4-5	304L	3274	0.0007*	No Reportable Corrosion
CAO2-5-6	304L	3275	0.0003*	No Reportable Corrosion
CAO2-2-6	316L	3368	0.0002*	No Reportable Corrosion
CAO2-3-8	316L	3369	0.0001*	No Reportable Corrosion
CAO2-5-1	316L	3370	0.0007*	No Reportable Corrosion
CAO2-6-3	316L	3371	0.0007*	No Reportable Corrosion
CAO2-2-1	316L Welded	W3676	Weight gain 0.0007*	No Reportable Corrosion
CAO2-3-3	316L Welded	W3677	Weight gain 0.0003*	No Reportable Corrosion
CAO2-3-5	316L Welded	W3678	Weight gain 0.0006*	No Reportable Corrosion
CAO2-5-5	316L Welded	W3679	Weight gain 0.0007*	No Reportable Corrosion
CAO2-1-1	Zircaloy-4	3796	Weight gain 0.0016	No Reportable Corrosion
CAO2-4-8	Zircaloy-4	3797	Weight gain 0.0011	No Reportable Corrosion
CAO2-6-1	Zircaloy-4	3798	Weight gain 0.0009	No Reportable Corrosion
CAO2-6-2	Zircaloy-4	3799	Weight gain 0.0010	No Reportable Corrosion

a. weight loss or gain (if any) is within the tolerance of the Mettler AE 163 Balance.

scale measurements, in some cases combined with uncertainties due to the wash/brush process). Note, also, that losses of base metal due to chemical cleaning of aluminum, beryllium, and carbon steel, as described in Section 3.4, have already been accounted for in the reported weight losses for coupons of those compositions. A discussion of significant results follows.

3.5.1 Aluminum

4-Ft Level

The corrosion rates ranged from no reportable corrosion to 0.0028 MPY (7.1 X 10^{-8} m/year) with no localized corrosion.

10-Ft Level

The corrosion rates ranged from no reportable corrosion to 0.0013 MPY (3.3 X 10^{-8} m/year) with no localized corrosion.

3.5.2 Beryllium

Unexposed

For reference purposes, Figure 14 shows an unexposed beryllium coupon that has gone through the cleaning cycle.

4-Ft Level

The coupons had corrosion rates that ranged from 0.025 to 0.111 MPY. All of the coupons were pitted.

10-Ft Level

The beryllium coupons had corrosion rates measured from 0.152 MPY to 0.202 MPY. One of the exposed coupons is shown in Figure 15 with a surface corrosion product. Figure 16 shows the same coupon after cleaning, with pitting being evident.

Pitting Measurement

The pitted areas of three beryllium coupons exposed at the four foot level were measured with vertical scanning-interferometry. This technique can map the surface of the samples and measure pit depth. The maximum pit depth measured was 153 μm (6 mil) on sample S / N – 1. A three dimensional plot of this pit is shown in Appendix C, page C-2.

3.5.3 Carbon Steel

4-Ft Level

The corrosion rates ranged from 0.11 MPY to 0.14 MPY. The coupons were pitted, as shown in Figure 17 and 18.

10-Ft Level

The corrosion rates for carbon steel ranged from 0.22 MPY to 0.28 MPY. The coupons were pitted.

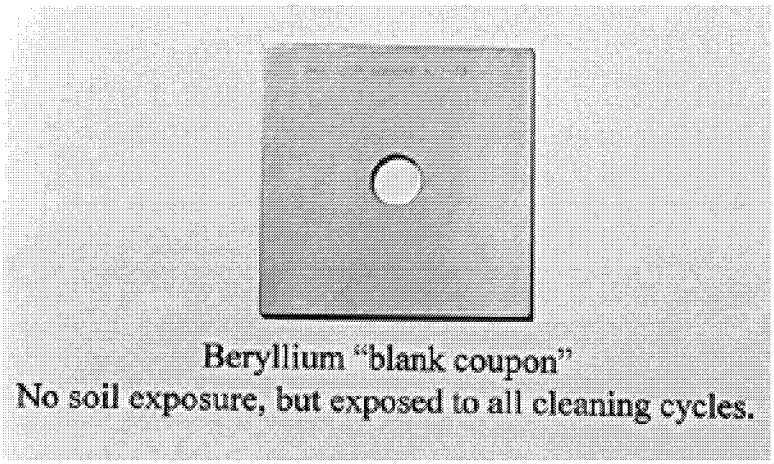

Figure 14. Beryllium blank coupon.

Figure 15. Beryllium coupon, after exposure, before cleaning

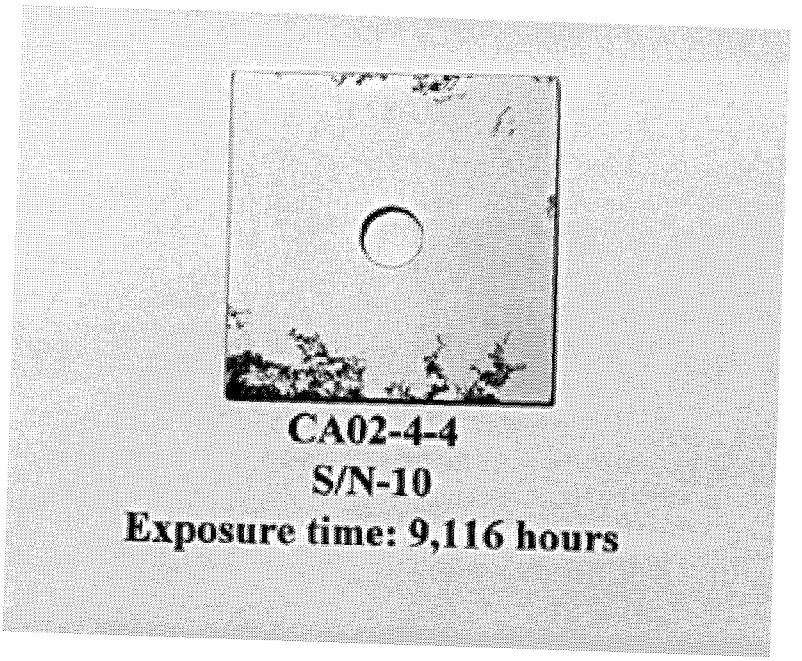

Figure 16. Beryllium coupon after cleaning.

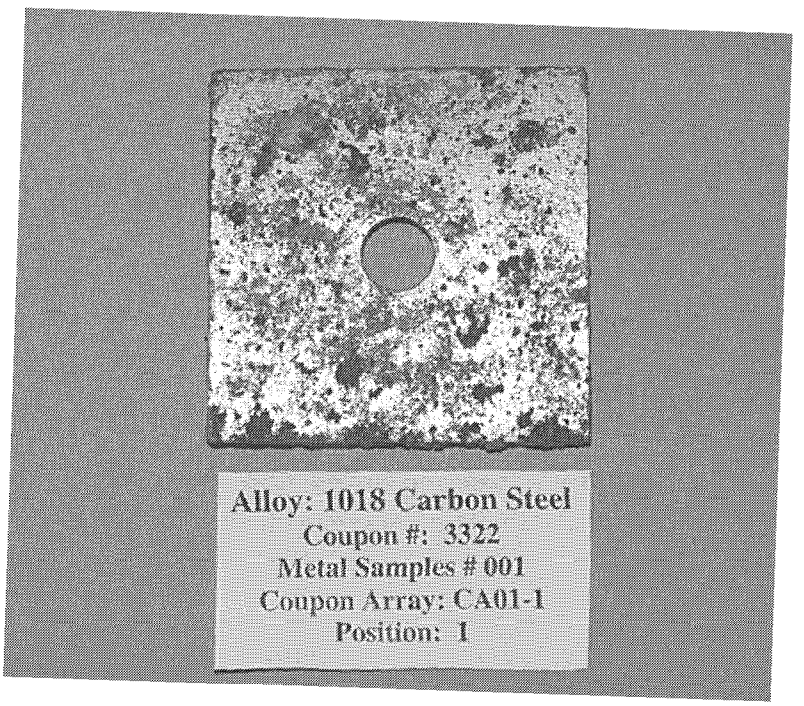

Figure 17. Carbon steel, after exposure, uncleaned

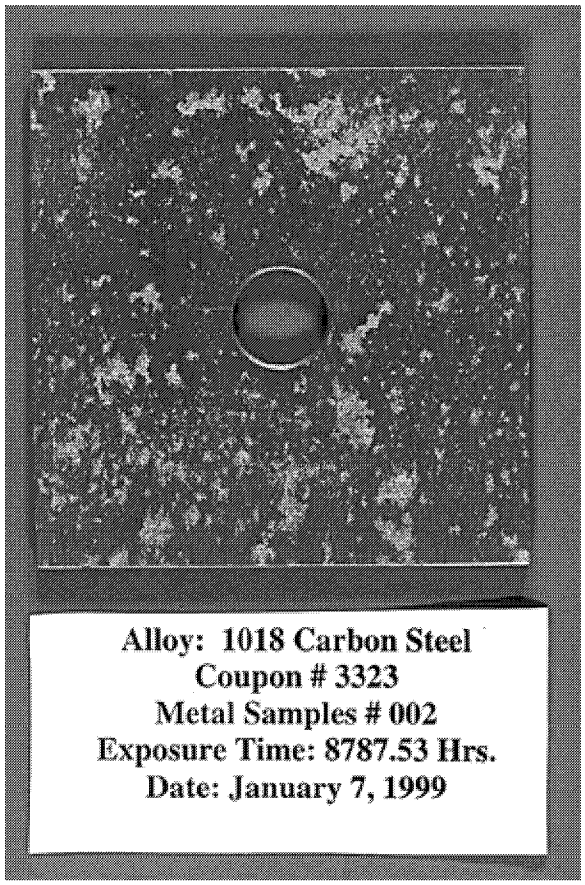

Figure 18. Carbon steel at the 4-ft level, cleaned.

Pitting Measurement

Nineteen pitted areas of the four carbon steel coupons exposed at the 4-ft level were measured with vertical scanning-interferometry. This technique can map the surface of the samples and measure pit depth. The maximum pit depth measured was 141μm (5.5 mil) on sample 3323. A three dimensional plot of this pit is shown in Appendix C, page C-1.

3.5.4 Other Metals

Coupons of the other six compositions (Ferralium 255, Inconel 718, 304L stainless steel, 316L stainless steel, 316L welded stainless steel, and Zircaloy-4) showed little or no evidence of corrosion. No signs of corrosion attack were visible on any of the coupons of these compositions. Most of the measured weight losses (if any) were lower than the reportable threshold, and the few weight losses that were reportable were very small. The very small weight gains measured on the Zircaloy-4 coupons are possibly due to the development of a very thin ZrO_2 corrosion film on the coupons (Hillner et al. 1994; Franklin 1997). This tentative explanation assumes that the wash/brush process was not successful at removing all of the corrosion film.

3.6 One-Year Coupon Weight Changes And Uncertainties

Table 8 summarizes the average measured weight losses after one year for sets of four coupons of each composition buried for corrosion testing. Included in the table are the balance uncertainties and the combined cleaning/balance uncertainties as determined in the coupon cleaning tests performed at the INEEL (Wilkins et al.), as described in Section 3.4 of this report. The aluminum and beryllium coupons are less dense than the other compositions and hence were measured on the balance in a lower weight range having a smaller error. Note that combined cleaning/balance uncertainties, applied to the one-year results, are given only for 304L and 316L stainless steels and Inconel 718, the only three compositions examined in the coupon cleaning tests (that is, the wash/brush process imposed on uncorroded coupons). It should also be noted that the 95% confidence level balance uncertainties in the table are simply twice the standard deviations (2σ) of the sets of balance measurements reported in the document cited above. This in accordance with NIST practice for uncertainty levels and their propagation.

Table 8. One-year coupon weight changes and measurement uncertainties.

Material Type	4-Ft Depth Average Weight Change (mg)	10-Ft Depth Average Weight Change (mg)	2σ Balance Uncertainty (mg)	2σ Cleaning + Balance Uncertainty (mg)
Aluminum	-0.98	-0.55	± 0.4	
Beryllium	-47.0	-109.8	± 0.4	
Carbon Steel	-312.2	-642.8	± 0.8	
Ferralium 225	-0.53	-1.0	± 0.8	
Inconel 718	+0.10	-0.05	± 0.8	± 0.92
304L	-0.08	-0.45	± 0.8	± 0.89
316L	-0.53	-0.43	± 0.8	± 0.98
316L Welded	+0.48	+0.58	± 0.8	
Zircaloy-4	+0.98	+1.15	± 0.8	

Two salient points are apparent in Table 8. First, the measured weight losses for the beryllium and carbon steel are much greater than those for any other coupon compositions. It is readily apparent in Table 8 that the average weight losses for those two compositions exceed the 2σ balance uncertainties by two or three orders of magnitude. (Interestingly, the weight losses at the 10-ft depth are approximately twice those at the 4-ft depth.) The lack of a combined cleaning/balance uncertainty leaves a gap in the data for the one material that may be of greatest interest in the one-year weight-loss measurements—beryllium. Without further testing, the contribution of the cleaning process to the uncertainty for the beryllium remains unknown. Determination of the beryllium cleaning uncertainty is thus a worthy goal that would add credibility to the beryllium corrosion rates.

Second, the average weight losses for nearly all the other compositions (that is, excluding beryllium and carbon steel) are of the same order of magnitude as, or smaller than, the 2σ balance uncertainty. Only the aluminum coupon set from the 4-foot depth does not fit that pattern, and among the four aluminum coupons in that set, only two do not fit the pattern. One aluminum coupon from the set buried at a 10-ft depth also had a weight loss somewhat larger than the balance uncertainty. Thus, excluding the beryllium and carbon steel, among a total of 56 coupons of seven compositions, only three had weight losses significantly larger than the measurement uncertainty of the balance used to determine those weight losses. The combined 2σ cleaning/balance uncertainty exceeded the average and individual coupon weight losses in all cases for the 304L, 316L, and Inconel 718 coupons, for both the 4- and 10-ft levels.

Figures 19 through 24 plot the individual coupon weight losses for 304L, 316L, and Inconel 718, with balance uncertainties and combined cleaning/balance uncertainties noted as error bands. These data plots illustrate the fact that for these compositions, the one-year weight losses are "buried in the noise." Figures 25 and 26 illustrate the individual beryllium weight losses with error bands for the balance uncertainties only.

It is significant that most of the one-year weight-loss measurements are of the same order of magnitude as the 2σ balance uncertainty. The corrosion results that fell within this uncertainty band were reported as "No reportable corrosion" in Tables 6 and 7.

The conclusion to be drawn from these results is that the actual corrosion rates at the SDA might be considerably lower than the standard corrosion rates developed by Oztunali and Roles (1986) and used by Maheras et al. (1994) in the SDA performance assessment. However, the testing conducted so far has been early-stage testing. The test conditions that have existed thus far have involved metals separated from each other in relatively dry soil. As has been intended from the beginning, the testing should be expanded to include higher moisture, higher temperature conditions, and to include dissimilar metals in contact with each other, as is actually the case with much of the metal buried at the SDA.

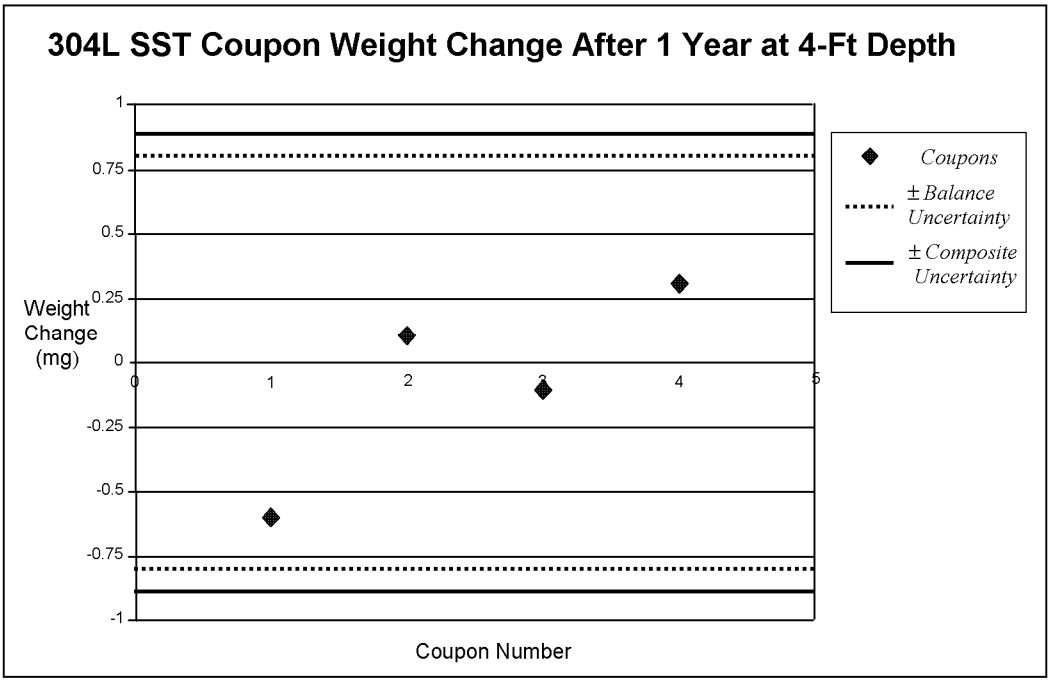

Figure 19. 4-ft depth – 304L weight change.

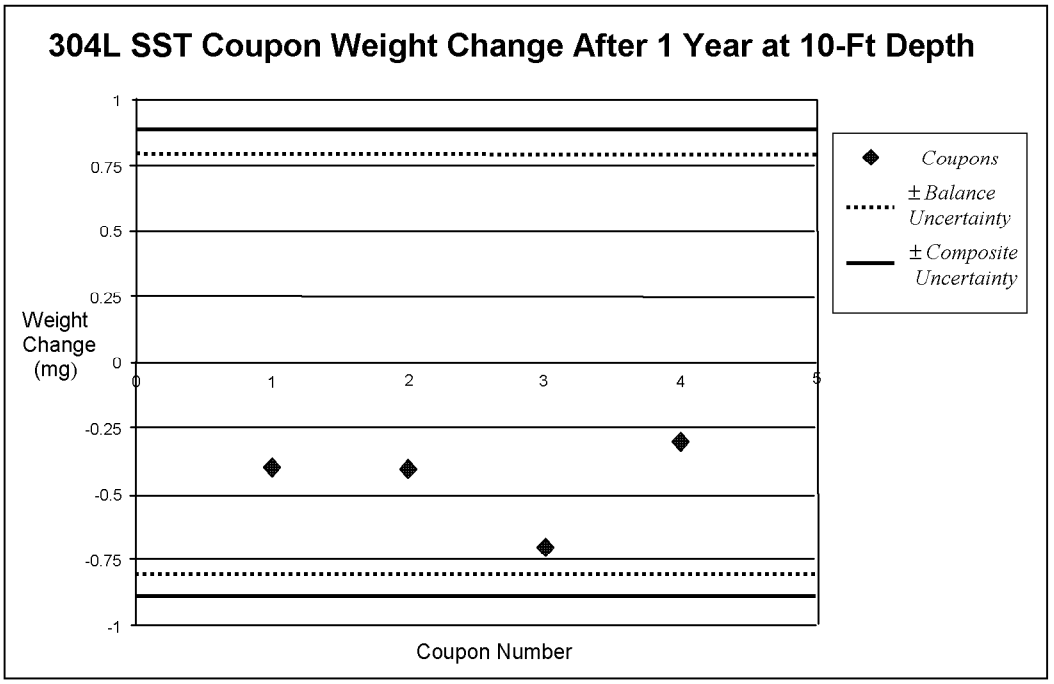

Figure 20. 10-ft depth – 304L weight change.

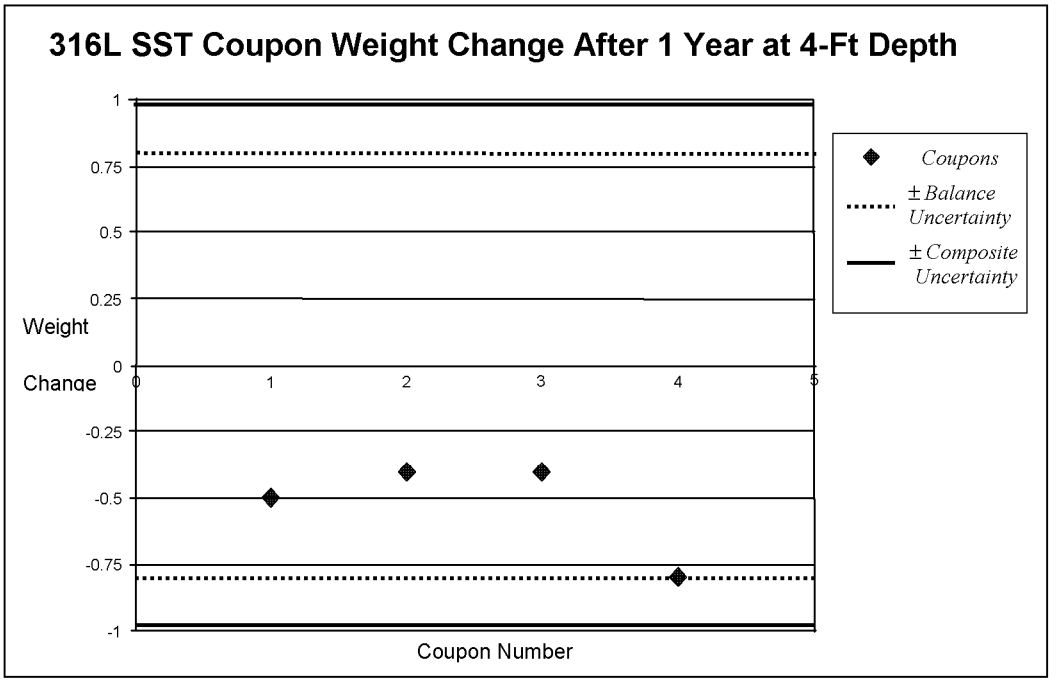

Figure 21. 4-ft depth – 316L weight change.

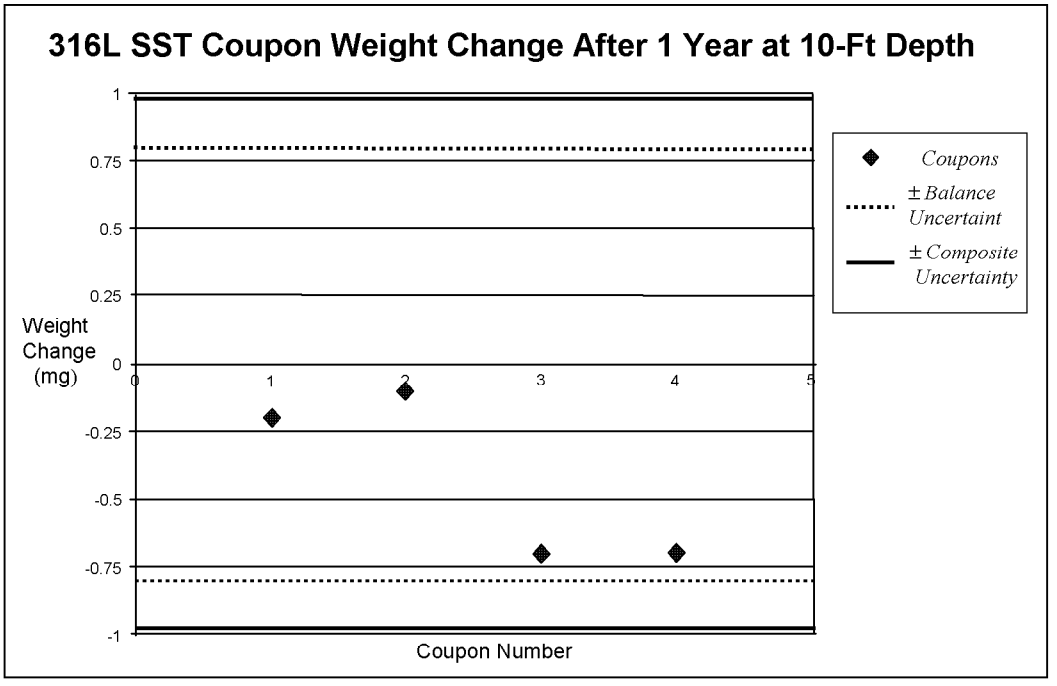

Figure 22. 10-ft depth – 316L weight change.

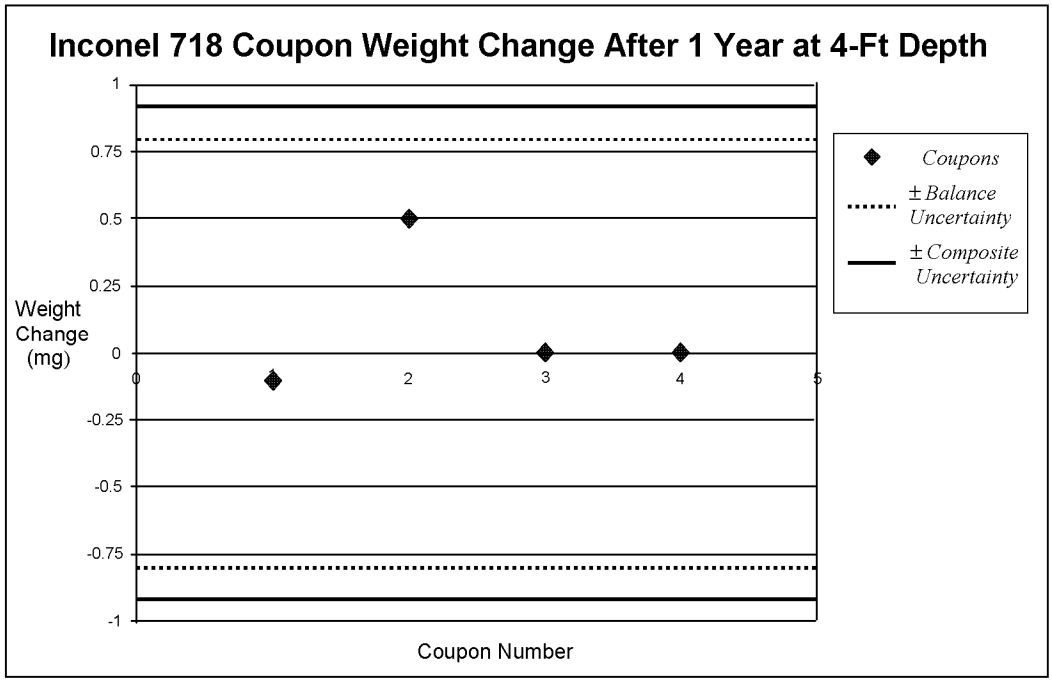

Figure 23. 4-ft depth – Inconel 718 weight change.

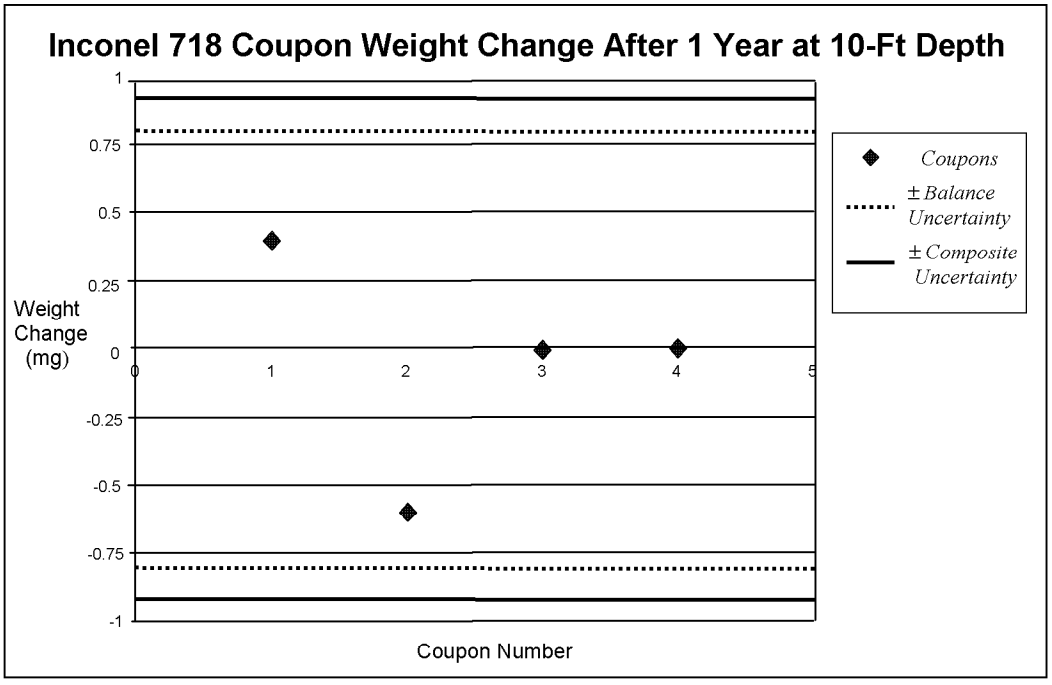

Figure 24. 10-ft depth – Inconel 718 weight change.

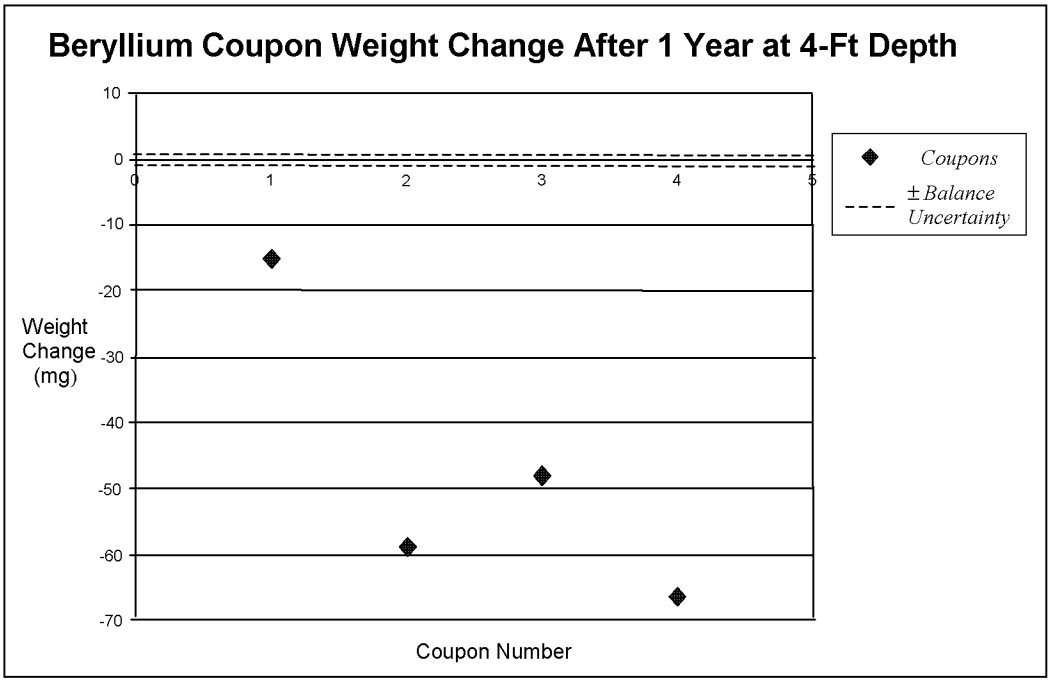

Figure 25. 4-ft depth – beryllium weight change.

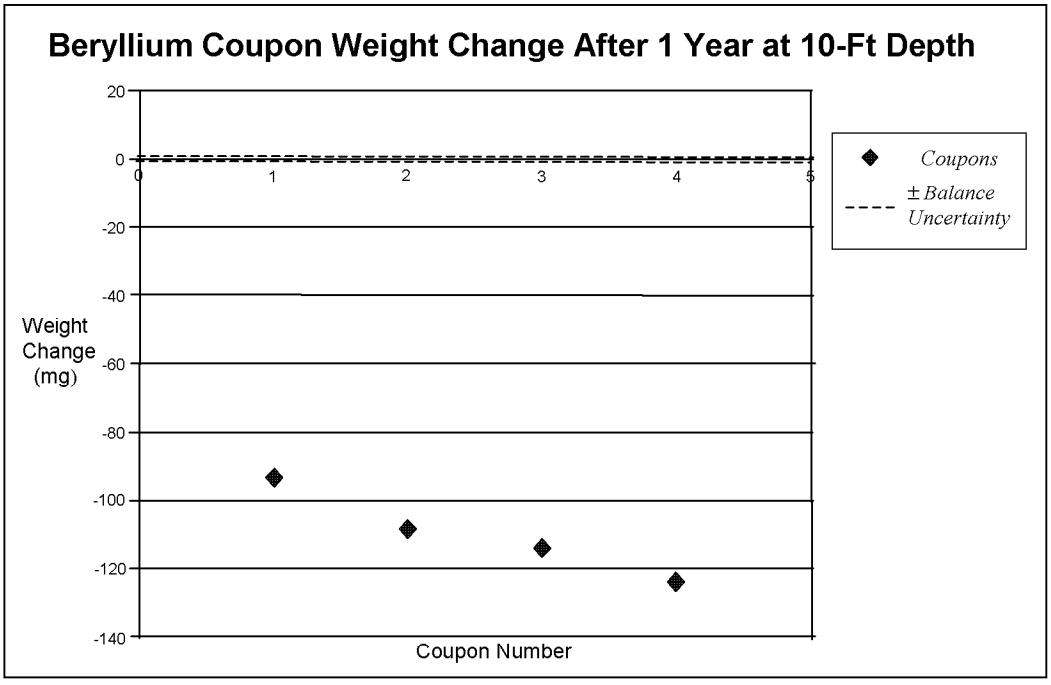

Figure 26. 10-ft depth – beryllium weight change.

4. RELATED STUDIES

4.1 Factors That Describe Soil Corrosivity

4.1.1 Soil Resistivity

The conductivity of the environment on the area of contact between underground metallic structures and the soil has been recognized as an important factor in the activity of the resultant corrosion cell. Soil resistivity is the reciprocal of conductivity and is a measure of the current carrying capacity of the soil. The resistivity of unsaturated soils depends primarily on the soil moisture content, electrical resistivity of the pore fluids, and to a lesser extent, the clay content (Tullis et al. 1993).

The results of a study by Palmer (1974, 1989) on the relationship between soil resistivity and corrosivity of buried carbon steel is shown in Table 9.

Table 9. Resistivity classifications for carbon steel pipe (Palmer 1974, 1989).

Resistivity Range (ohm-cm)	Corrosivity
0 - 1000	Very severe
1001 - 2000	Severe
2001 - 5000	Moderate
5001 - 10,000	Mild
10,001 -	Very mild

The soil resistivity of the Spreading Area B soils was measured by Tullis et al. in the borrow pit using the Four Electrode Wenner array (ASTM G 57) and reported as 8,500-10,000 ohm-cm. The measured values for the Spreading Area B soil put it into the mildly corrosive category, as shown in Table 9. A comparison of soil resistivities and corrosion rates at various sites that have performed underground corrosion tests is shown in Table 10.

Table 10. Soil resistivity and corrosion rate of stainless steel.

Resistivity (ohm-cm)	Corrosivity (Palmer 1974)	Test Site	Resistivity (ASTM G57) (ohm-cm)	Corrosion Rate (MPY) 304/304L stainless steel
0 – 1,000	very severe	Toppenish WA	400 [a]	3.9×10^{-4} (8.2 years @ 2.5 ft)
1001-2000	severe			
2,000-5,000	moderate	INEEL	2600-2700[b]	No Reportable Corrosion
5,001-10,000	mild	INEEL	8,500-10,000 [c]	No Reportable Corrosion
>10,000	very mild	Hanford	50,000	2.1×10^{-2} (1 year @ 10 ft)

a. Gerhold et al. 1976

b. Pfeifer 1997

c. Tullis et al. 1993

4.1.2 Soil pH

The standard method for in-situ soil pH measurements, ASTM G-51, requires a good liquid junction between the pH electrode and the test soil. Due to the low moisture content in the Spreading Area B soil, this method was not used.

Samples of Spreading Area B soils were analyzed for pH using the methods described by Black et al. (1965), and the results were reported by Tullis et al. (1993). The pH of Spreading Area B Soil is mildly alkaline (pH 8.1 to 8.3). This pH would generally be expected to form a passive film on the carbon steel and stainless alloys.

An analysis by Durr and Beavers (1998) looked at the combined effect of pH and resistivity on corrosion of carbon steel in soil above the water table. The study used published data to plot the corrosion versus the product of the pH and the log of the soil resistivity. Using the INEEL values of pH 8.2 and a resistivity of 5,000 ohm-cm, we get a corrosion rate of 0.1 MPY, which compares favorably with the average carbon steel INEEL rates (after one year exposure) of 0.12 MPY at 4 ft and 0.25 MPY at 10 ft.

4.1.3 Soil Type/Moisture

The SDA and the corrosion test site are located in a vadose zone that consists of fine-grained aeolian deposited sediments. Tullis et al. (1993) describe the Spreading Area B soils as being composed of primary loess deposition and loess erosion and redeposition. The soil texture is a silty loam with a maximum clay component of approximately 25%. It is expected that the soil in the test Berm is free of stratification.

Section 4.2 describes soil moisture monitoring at the test Berm and discusses those results in relation to what is known about soil moisture at the SDA. That discussion raises several issues with the soil moisture measurement and how well the Berm models the SDA. The following paragraph summarizes.

First, the moisture conditions at the Berm may not conservatively represent moisture conditions at the SDA. The SDA can be affected by ponding of water with spring snowmelt or heavy rainstorms. Second, neutron probe access tubes placed in the Berm might not accurately measure moisture infiltration in the 6-ft-diameter holes drilled into the Berm to install the coupons. The backfill in the 6-ft-diameter holes is not compacted as much as the soil in the bulk of the Berm, and the drilling operation compacts the soil around the circumference of the 6-ft-diameter drill hole for the entire depth. These conditions might lead to non-uniform moisture conditions between the bulk of the soil in the Berm and the soil in contact with the corrosion coupons. Additional information about these issues is provided in Section 4.2.

4.1.4 Soluble Ion Concentration

The underground corrosion of metals will be affected by soluble ions present in the soil (Piciulo et al. 1985; Chaker 1995; Durr and Beavers 1998). Soluble ions present in the Spreading Area B soils are included in the discussion in Section 4.1.5 of this report. Generally accepted is that the presence of chloride ions will be detrimental to stainless steels, aiding corrosion and decreasing resistance to pitting. Although there is no underground corrosion data available on beryllium, corrosion tests performed in natural seawater and NaCl solutions pitted the beryllium.

The soluble ion concentration can increase the soil conductivity (reduce the resistivity), which will increase the corrosivity. In a study cited by Durr and Beavers (1998), increasing concentrations of $CaSO_4$ and NaCl in solutions decreased the soil resistivity (Figure 27).

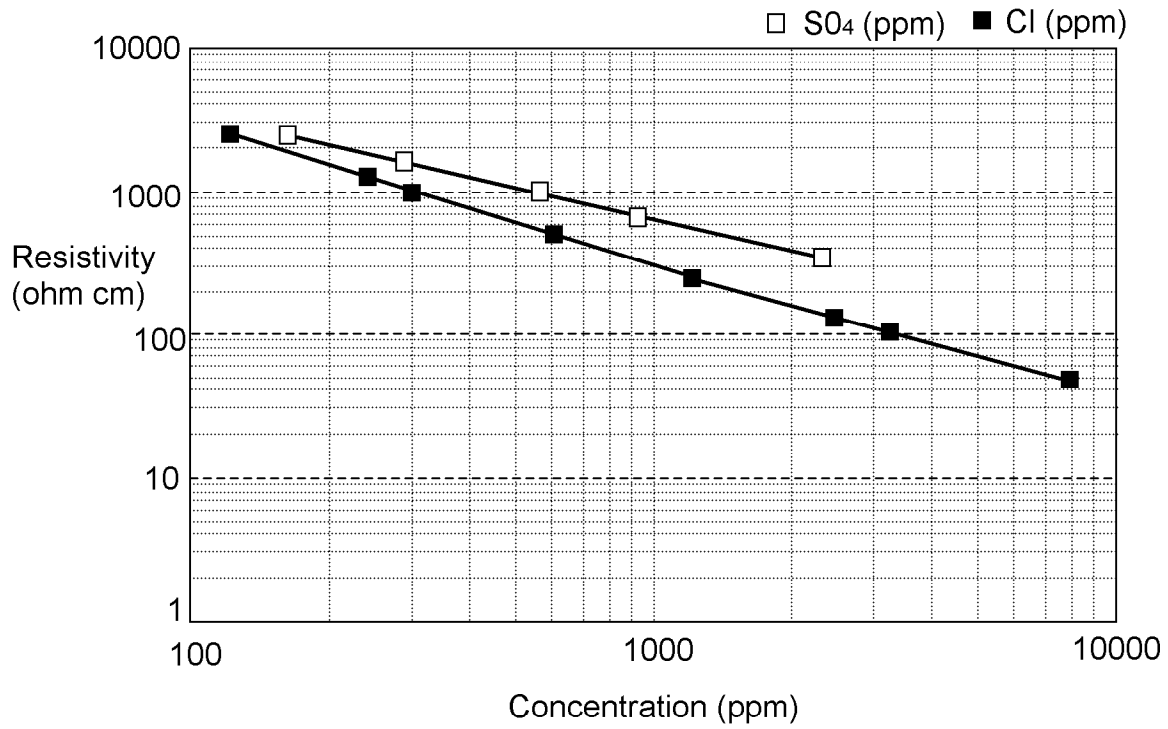

Figure 27. Resistivity as a function of $CaSO_4$ and NaCl solutions.

4.1.5 Comparison With Other Sites

The results of underground corrosion tests performed by Gerhold et al. (1976) for the National Bureau of Standards (NBS), now the National Institute for Standards Testing (NIST), are shown in Table 11. The Gerhold measurements were from exposure to Sagemoor Sandy Loam soil located at the Yakima Indian Reservation, Toppenish, Washington. The Sagemoor Sandy Loam soil is characterized as a well-drained alkaline soil with a resistivity of 400 ohm-cm and a pH of 8.8. It is typical of soils found in eastern Washington and Oregon.

As can be seen, the corrosion rates for annealed and as-welded material are extremely low. The corrosion rates from the NBS study do not correlate well with data from Palmer (1974) on the relationship of resistivity and the corrosion rate of carbon steel.

Corrosion testing was performed at the Hanford site at the 200 West Area. Carbon and stainless steel corrosion samples were buried at depths of up to 30 ft. The soil is characterized as wind blown loess down to a level of about 4 ft, with an underlying layer of Hanford formation sediments (Bunnel et al, 1994). The corrosion rates for exposures of up to two years are given in Table12.

The Hanford results are compared to the INEEL results in Table 13. The corrosion rate for stainless steel at the INEEL was essentially non-detectable for the one-year test period. The results of soil analyses, including soluble ions, for the Hanford Site and for the Spreading Area B soils at the INEEL, are shown in Table 14.

Table 11. Results for stainless steels exposed to Sagemoor sandy loam soils.

Material	Sample Form	Treatment	Exposure Time Days	Weight Loss mg/dm^2	Corrosion Rate mils/year
304	sheet	annealed	2989	8	3.9×10^{-4}
304	sheet	sensitized	413	20	6.9×10^{-3}
			791	18	3.3×10^{-3}
			1442	49	4.9×10^{-3}
			2989	68	3.3×10^{-3}
304	welded sheet	as-welded	2989	17	8.2×10^{-4}
316	sheet	annealed	2989	0.0	0
316	sheet	sensitized	791	5	9.1×10^{-4}
			1442	31	5.7×10^{-4}
			2989	12	5.8×10^{-4}

Table 12. Results from the Hanford site.

Material	Burial Depth (Ft.)	Corrosion Rate (MPY)			
		9 months	1 Year	2 Years	Average
Carbon Steel					
	5	1.7	-	-	1.7
	10	0.9	1.0	1.4	1.1
	15	-	-	1.0	1.0
	20	0.3	0.6	0.4	0.4
	30	-	0.2	0.6	0.4
Stainless Steel (304L)					
	5	0.0065	-	-	0.0065
	10	0.0096	0.0210	0.0029	0.0012
	15	-	-	0.0036	0.0036
	20	-	0.0180	0.0075	0.0127
	30	-	0.0190	0.0049	0.0119

Table 13. Site comparisons.

Material	Location	Burial Depth (Feet)	Corrosion Rate (MPY)	
			9 months	1 year
Carbon Steel	Hanford Site	5	1.7	-
		10	0.9	1.0
	INEEL	4	-	0.125
		10	-	0.25
Stainless Steel 304L-annealed	Hanford Site	5	0.0065	-
		10	0.0096	0.0210
	INEEL	4	-	No Reportable
		10	-	No Reportable

Table 14. Comparison of soil analyses from INEEL and Hanford Site.[a]

DATA	INEEL	HANFORD SITE
Resistivity: Wenner array ohm-cm.	10,000	-
Resistivity: Miller box ohm-cm.(saturated)	2,750-4,500	16,000
Moisture content (%)	3.45-13.7	0.67-6.49
Soil pH (in 0.01M $CaCl_2$)	8.1-8.3	7.08-7.66
Acidity (meq/100 g)	3.4-16.2	2-4
Soluble Ions (meq/100 g)		
Calcium (Ca^{-2})	0.11-0.25	0.0039-0.0082
Magnesium (Mg^{+2})	0.07-0.26	0.0045-0.033
Potassium (K^{+})	0.004-0.01	0.0022-0.011
Sodium (Na^{+})	0.028-0.05	0.0055-0.18
Carbonate (CO_3^{-2})	ND	-
Bicarbonate (HCO_3^{-1})	0.10-0.29	0.013-0.086
Sulfate (SO_4^{-2})	0.02-0.05	0.004-0.042
Sulfide (S^{-2})	ND	ND-0.00025
Chloride (Cl^{-})	0.006-0.02	0.00096-0.16
Exchangeable cations (meq/100 g)		
Calcium (Ca^{2+})	14.1-44.1	6.7-26.0
Magnesium (Mg^{2+})	3.94-11.9	0.91-2.1
Potassium (K^{+})	0.54-1.19	1.4-9.6
Sodium (Na^{+})	0.09-0.22	0.072-1.0
Cation Exchange Capacity (meq/100 g)		
Exchangeable Bases	19.05-57.41	19
Exchangeable acidity	3.4-16.2	2
Cation exchange capacity	27.1-50.4	21

a. From Tullis, et al.

4.2 Corrosion In Similar Soils

An earlier study performed at the INEEL by Nagata and Banaee (1996) used literature sources to estimate the corrosion rates for low carbon steels, Types 304 and 316 stainless steels, and Inconel 600, 601, and 718 alloys in SDA-type soils. The study compared those estimates to the corrosion rates specified in the SDA performance assessment (Maheras et al. 1994), which were based on the IMPACTS study (Oztunali and Roles 1986). The results of the INEEL study by Nagata and Banaee are summarized here. The study made the following assumptions:

- The underground corrosion behavior of Type 304 stainless steel at the SDA can be estimated by the behavior of Type 304 stainless steel in similar soils.

- The corrosion behavior of neutron-irradiated metals is not very different from that of their unirradiated state; that is, the concentration of activation products is so small that they do not significantly change the chemical composition, and hence the corrosion behavior, of the alloy.

- The activated elements in the neutron-irradiated metals are uniformly distributed, so the uniform corrosion rate describes the release of the activated elements to the environment. (The uniform corrosion rate, for "corrosion that proceeds at about the same rate over a metal surface," is used because the volume of metal corroded determines the release of radionuclides to the environment. Therefore, even if corrosion proceeds by pitting, as it does for austenitic stainless steel in underground corrosion, the uniform corrosion rate is always reported because the loss in metal volume to pitting cannot be easily measured, whereas the uniform corrosion rate can. Furthermore, if the concentration of the activated elements is fairly uniform, the mechanism of metal loss, i.e., by pitting or uniform corrosion, is unimportant; only the volume lost is important.)

The study estimated that the corrosion rate for the stainless steels and Inconels in environments with geochemistry similar to that of the SDA soils was 0.00047 MPY (1.2×10^{-8} m/year), which is about two orders of magnitude lower than the corrosion rates specified in the SDA performance assessment for stainless steel. The study considered the corrosion rate for Inconel 718 to be the same as for the austenitic stainless steels.

4.3 Soil Moisture Testing at the Test Berm

4.3.1 Hydrologic Setting

The hydrologic setting for the corrosion test is an important parameter that affects corrosion; evaluated soil moisture and water table position have been found to be correlated with increased corrosion (Durr and Beavers 1998). The potential impact of hydrology on the corrosion rates of the coupons is evaluated in the following discussion.

The Berm where the corrosion testing is being conducted is located in the vadose zone approximately 177 m (580 ft) above the Snake River Plane aquifer in southeastern Idaho. The vadose zone consists of 3 to 6 m (10 to 20 ft) of fine-grained aeolian deposited sediments overlaying hundreds of feet of thin basalt flows containing occasional sedimentary interbeds and rubble zones. The aquifer is located in yet deeper basalt flows.

On average, the region where the Berm is located receives 21.97 cm (8.65 in.) of precipitation a year (National Oceanic and Atmospheric Administration records). Spring and summer rainstorms generally supply most of the precipitation, but soil moisture and total infiltration are impacted greatest by moisture supplied by snowmelt. Snowmelt at the Berm generally occurs in February and March, at a time that the water is free to infiltrate into the ground with little opportunity for evapotranspiration. The impact of snowmelt on infiltration is increased in areas where the water collects and is lessened in areas where the water runs off.

Precipitation is measured on the Berm with an all-weather rain gauge at the northeast corner of the EBTF. Precipitation measured at the Berm for the 1997-1998 period is shown in Figure 28. Total precipitation for the year was 22.52 cm (8.86 in.). The two largest events occurred on May 12, 1998 (2.1 in.) and September 12, 1998 (2.0 in.). If the assumption is made that precipitation that occurred in November, December, January, and February fell as snow, then 3.95 cm (1.56 in.) of the precipitation was snow while 18.57 cm (7.31 in.) occurred as rain.

4.3.2 Moisture Monitoring

Three 3-m (10-ft) neutron probe access tubes were installed in the test berm near the coupon burial sites (Figure 29) for the purpose of monitoring soil moisture. The neutron probe access tubes are designated on Figure 29 as NP1, NP2, and NP3. Moisture monitoring was initiated in January of 1998 and continued through October 1998.

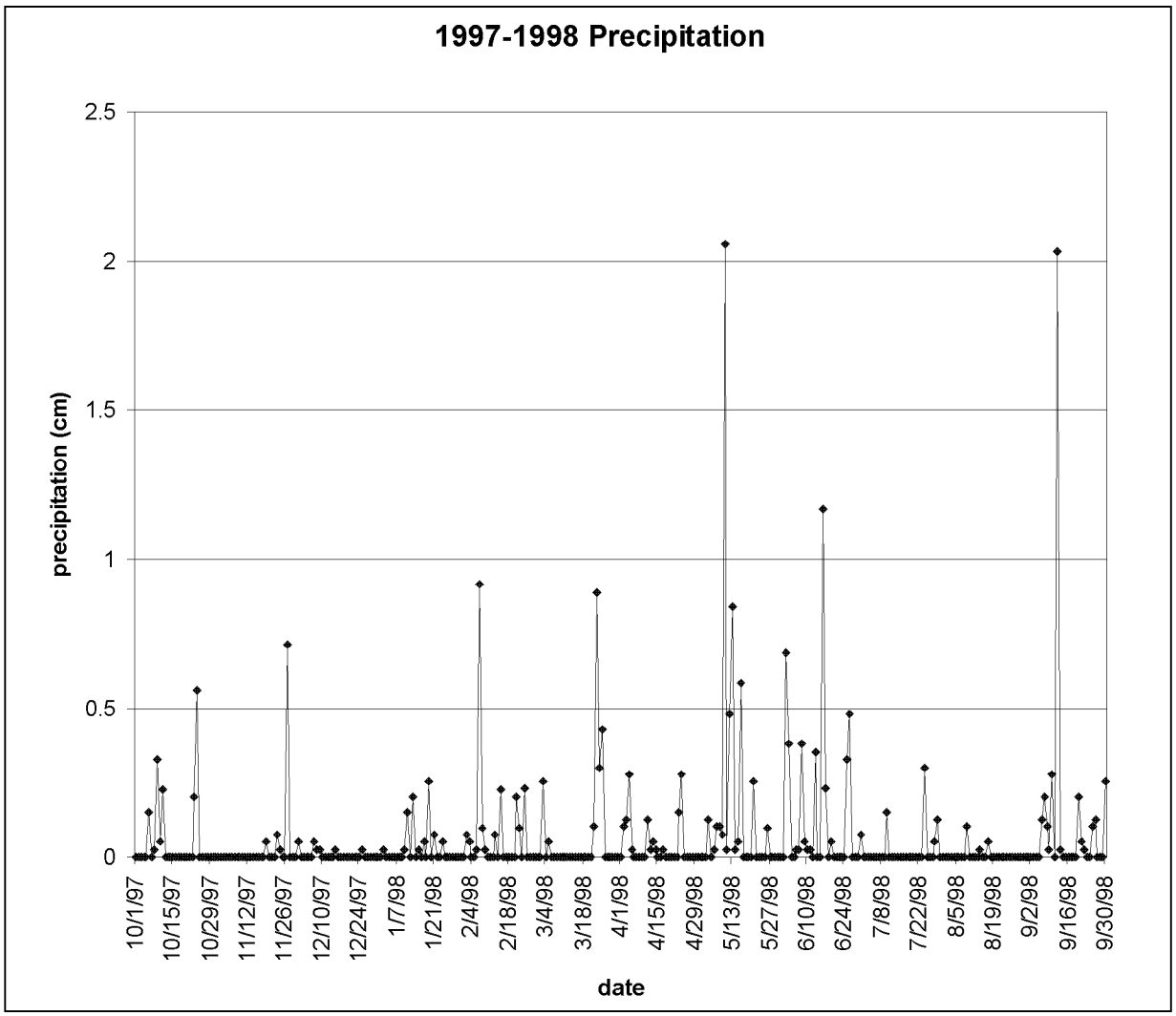

Figure 28. Measured precipitation.

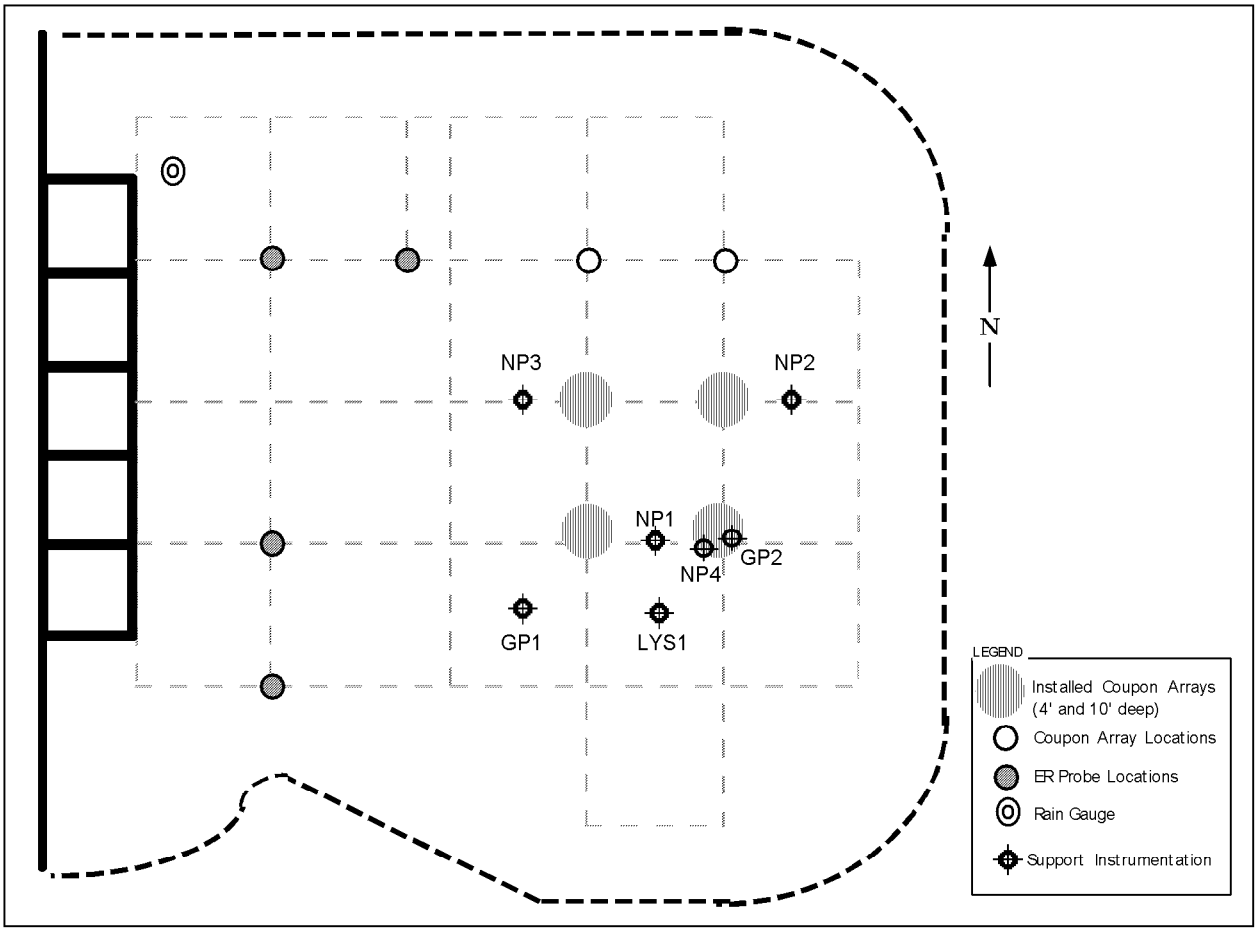

Figure 29. Installation locations of neutron probe access tubes and other support.

The tubes were installed by drilling a 2-in. auger hole, placing a 1.9-in. (outer diameter) stainless steel casing down hole, and filling the annular space with sieved native sediments. The backfill was packed into the annular space to ensure that the neutron monitoring tube did not become a conduit for moisture movement into the Berm. The installation was outside the 6-ft diameter holes drilled for the coupon installation.

4.3.2.1 Neutron Probe Operation. A CPN 503DR hydroprobe neutron moisture gauge with a 50 mCi Am/Be source was used to collect the moisture data. The gauge operates by emitting fast neutrons that are thermalized or slowed when they contact hydrogen atoms. The probe detector counts the thermalized neutrons, and the neutron counts are calibrated to the specific soil to indicate the moisture content.

Logging is initiated by lowering the source to the bottom of the hole where the first 16-second measurement is taken. The source is pulled up 6 inches and another measurement is taken. The process is repeated in 6-in. increments until the entire hole is logged. The source is about 12 in. long and must be in the subsurface for measurements to be safely taken, so the top 1.5 ft of soil is not measured nor is the bottom 6 inches. When the following discussion refers to surface moisture conditions, it is referring to the soil that is located 1.5 ft beneath the surface. And, likewise, the bottom of the hole is the measurement taken at 9.5 ft.

4.3.3 Monitoring Results

Figures 30, 31, and 32 show plots of the monitoring data for the neutron probe access holes designated NP1, NP2, and NP3, respectively. NP1 is closest to Location I, that is, the location of the corrosion coupon installations that were removed in October 1998.

4.3.3.1 NP1. In Figure 30, there are essentially two moisture profiles for the near surface soil—the wetter profile (January through July profiles) and a drier profile (September and October). From about 5.5 ft down to the bottom of the hole, the profile is essentially unchanged. The January 13, 1998 shows that the soil moisture content at the surface was fairly moist, plotting in the middle of the wetter profile. The wettest surface measurements were collected in June. After that time the surface began to dry out, and the driest surface measurements, 15% (volumetric moisture content), were taken in September and October. The September profile shows a drying pattern that extends down into the subsurface to about 6 feet. However, the October profile shows slight wetting from about 3.5 to 6 feet. This is likely a response to the September 12, 1998 rainstorm (see Figure 28).

Volumetric moisture contents at the 4-ft depth average about 23% for the wetter period and fall back to 21.5% for the drier profiles. However, soil moisture at the 10-ft depth remained relatively unchanged, with an average content of about 24%.

If all other parameters effecting corrosion were equal, the NP1 moisture monitoring profiles would suggest that the coupons at the 10-ft depth would experience more corrosion than those at the 4-ft depth, because they are exposed to more moisture for a greater length of time.

4.3.3.2 NP2. Figure 31 shows moisture profiles obtained from NP2, which is northeast of Location I. NP2 was monitored for the same time intervals as NP1, and the profiles are similar to those obtained from NP1.

The wettest near-surface profiles were measured on June 23 and July 7. The September profile shows a decrease in soil moisture from about the 6-ft level to the surface. The October profile is slightly wetter in the 4- to 6-ft range, as was also observed in the NP1 profiles.

4.3.3.3 NP3. NP3 moisture monitoring results are shown in Figure 32. NP3 is located to the northwest of Location I. It is closer to the center of the Berm than the other monitoring sites.

NP3 monitoring results are more scattered at the surface than either NP1 or NP2. This may be a result of its location near the berm center, away from the sides where the water tends to run off. This would result in a greater moisture supply, a conjecture that is supported by the measurements. The initial measurement collected on January 13, 1998 (Figure 32) shows a surface moisture content of about 17 %. Subsequent profiles show the top part of the berm (~4 to 1.5 ft) wetting up to 23% on June 1, 1998. The June 23 and following measurements show a gradual drying out of the surface. Moisture contents measured in the soils at the bottom of the tube tend to cluster around a 23% volumetric moisture content.

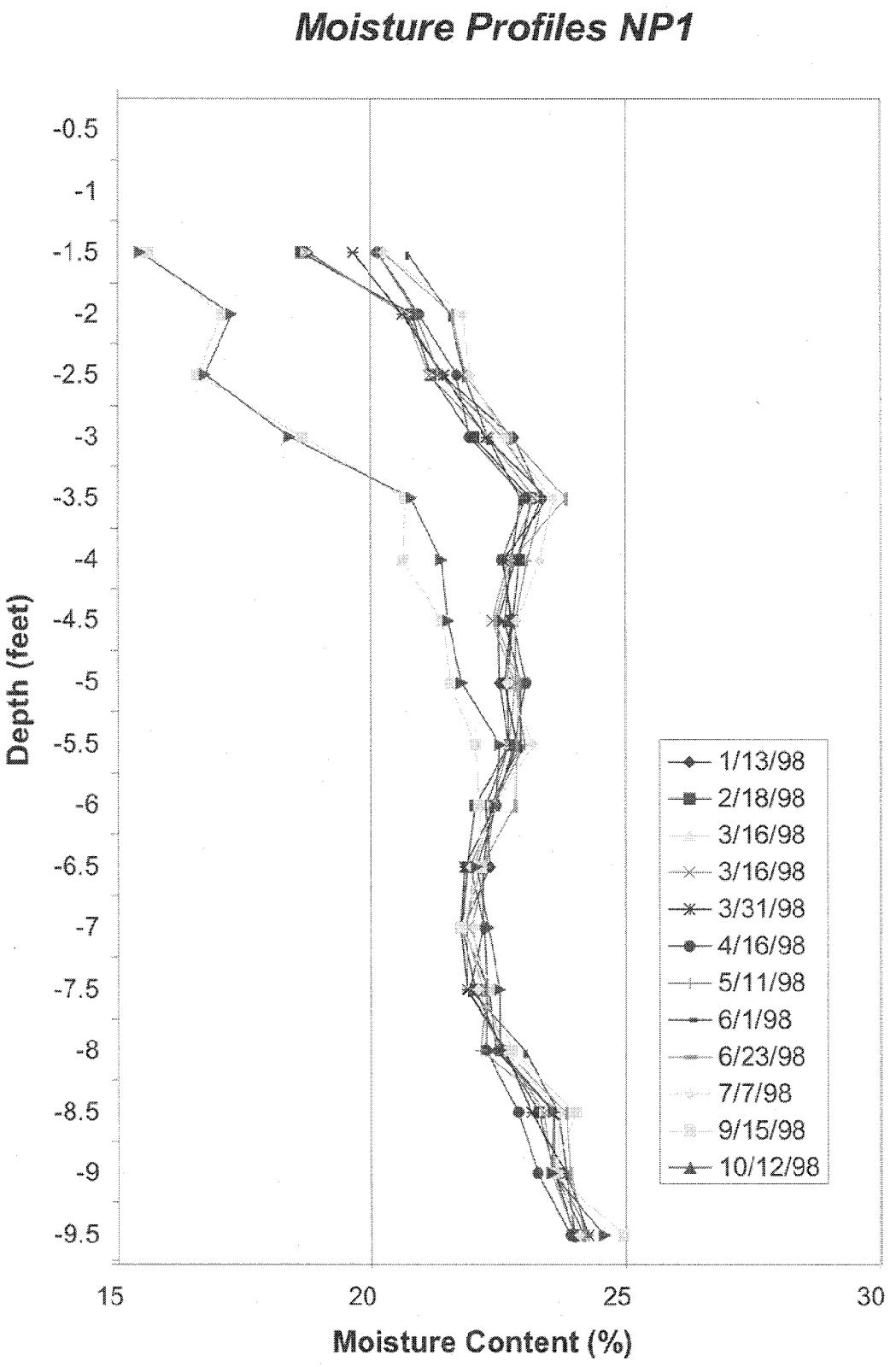

Figure 30. Moisture profile of NP1.

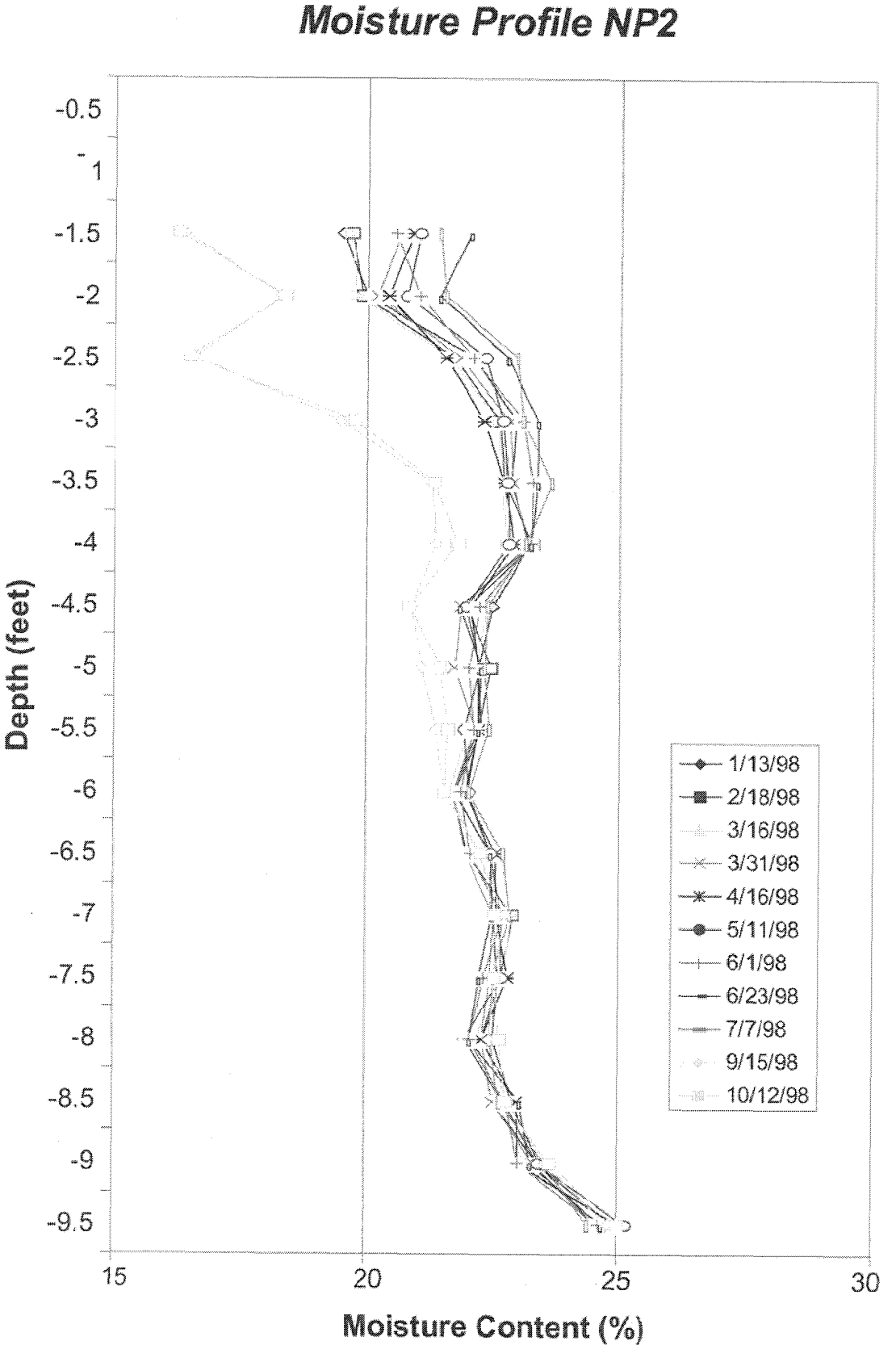

Figure 31. Moisture profile of NP2.

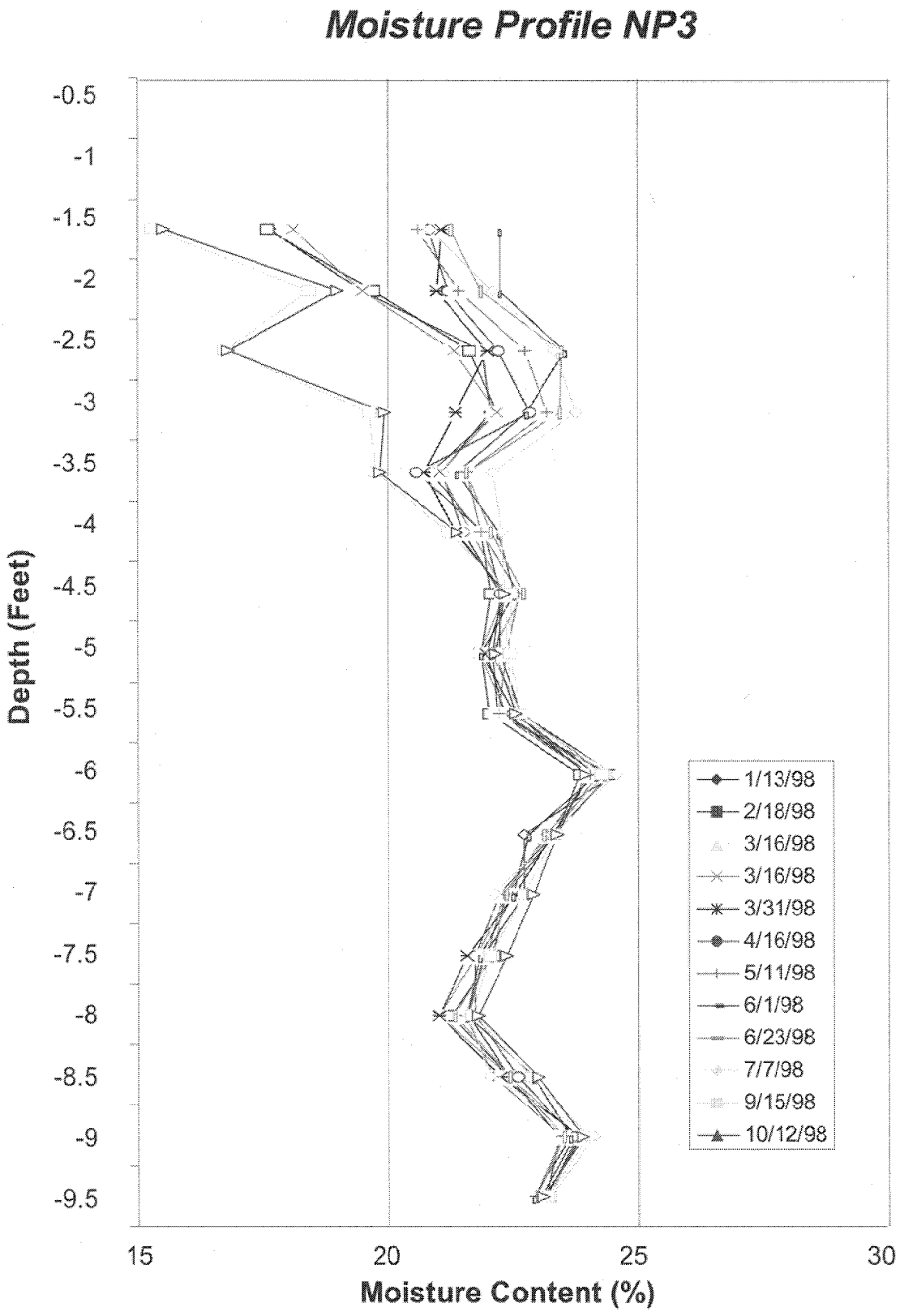

Figure 32. Moisture profile of NP3.

4.3.4 Discussion of Results

Two significant issues with respect to moisture are discussed in the following paragraphs.

First, the moisture profile data are slightly unusual because they show only slight infiltration and a large amount of drying out. Soil moisture profiles generally are more balanced than these with respect to the wetting and drying cycles; the unusual result shown here indicates that the soil is not at equilibrium with the current moisture regime. This likely results from one or both of the following scenarios: the berm soils were collected from an area where they received more moisture than at their current location or water was added during berm construction to obtain compaction. This means that the soils will continue to dry until they come to equilibrium with the current moisture regime. The current dry moisture regime is caused by the compacted nature of the berm, its relatively flat surface, and the tendency of precipitation to run off the berm rather than infiltrate. Precipitation that falls on the berm has been observed to collect in low areas and run off the berm, forming 8- to 10-in. deep erosion channels in the berm sides. NP3 shows the greatest infiltration, probably because it is located away from the berm edges and more of the precipitation is available to infiltrate into the soil rather than run off.

The test berm was developed as an analog for the SDA. Moisture contents in the SDA surficial sediments vary over a wide range depending upon location and time of the year (Bishop 1998). Infiltration in certain "dry" areas of the SDA may correlate with the berm conditions, but many area in the SDA are significantly more moist. Therefore, moisture conditions at the corrosion berm do not conservatively represent moisture conditions at the SDA.

Second, neutron probe access tubes placed in the Berm might not accurately measure moisture infiltration in the 6-ft holes drilled and backfilled at the Berm during installation of the coupons. The holes were installed with a 6-ft auger that tended to displace the subsurface soils resulting in 1- to 2-in. thick "walls." Additionally, when the holes were repacked during coupon emplacement, the resulting soil density was less than in undisturbed areas of the Berm.

The "walls" and the decreased density may result in a different moisture regime at the coupon installation locations than in the undisturbed Berm. Because soil moisture is still attempting to come to equilibrium with the current moisture regime, the differing moisture regimes are likely to have a greater impact on future coupon removal and analysis than on the coupons removed after one year of exposure. However, to verify that moisture contents in the Berm were the same (or different and quantify the difference) as in the soils surrounding the coupons, an additional neutron probe access tube was installed inside the 6-ft hole at location I (see Figure 4, presented earlier in this report). Results from monitoring that location will be reported when they become available.

An attempt was made to break up the "walls" during the most recent coupon placement (that is, installation of coupon arrays CA09 and CA10 in the hole from which the one-year coupons, CA01 and CA02, were removed). Rootlets were observed to concentrate at the wall interface, which was inferred to be an indication that more moisture was available at the interface.

4.4 Microbial Sampling

As part of the first year corrosion analysis effort, tests were conducted to identify microbes that were present on the coupons and in the surrounding soil. The results are intended to support efforts to determine whether these microbes are influencing the corrosion reactions.

There are several parameters that can be considered when attempting to detect microbial activity in soil systems. They include: isolation of colony forming units; content of select gases in the soil

atmosphere; soil moisture content; availability and type of electron acceptors; soil solution pH; soil temperature; nutrient supply; and available microbial inhibitors.

For this study, isolation of microbes and analysis of soil atmospheres were used as indicators of microbial activity associated with the buried coupons. Activity, then, was assessed both directly (isolation and culturing of microorganism obtained from the soil and from the surface of recovered coupons) and indirectly (analysis of the soil atmosphere).

4.4.1 Sampling Methods

The most direct method for determining numbers and types of viable microbes present in the soil environment is through the attempt to isolate and grow them on artificial media. Then by conducting an elementary morphological examination of the isolates, it is possible to gain a knowledge of the broad spectrum of microbial types (i.e. bacteria, fungi, and actinomycetes) present in the soil sample. Generally, exacting biochemical tests can be used (depending on available resources) to identify the genus and species of microbes. The tests can also be tailored to identifying a few general classes of microbes (i.e., aerobes, anaerobes, heterotrophes, autotrophes) of specific interest. The tests can be as exacting as the program budget will allow.

The methods described above can also be used to detect the presence of soil microbes that are associated with material buried in a soil profile. Once again, the methods used can be as involved as need and resources dictate. That can range from simply swabbing the surface and then conducting isolation work, to preparing the surface of interest and then subjecting it to visual and electron microscopic examination. Swabbing is a rapid method used to confirm the presence of microbes adhering to the surface. Visual and electron microscopy is particularly important when there is an interest in knowing if the attached microbes are involved with visible surface effects such as corrosion. Typically, such involved examinations are conducted after the presence of microbes and corrosion has been indicated by initial examination.

This study isolated and cultured microorganisms from the surfaces of selected coupons, from the Teflon identification tags, and from the adjacent soil. The microbial sampling technique used in this study is described in Appendix B. The results are presented in the following paragraphs.

The presence of microbes using solid media (agar plates) and selective liquid media (serum bottles) was confirmed within 48 hours. Solid media were of two types: nutrient agar with glucose (NAG), and phenol red agar with glucose (PRG). The results from the solid media are presented in Table 15. In general, the results from the microbial isolation effort showed that there were microorganisms present on the surface of all examined coupons. They included bacteria, actinomycetes, and fungi. While no effort was made to determine the numbers of microbes (i.e., enumeration by serial dilutions), growth on those areas of agar imprinted with the surface of each coupon was very heavy. In addition, imprints of Teflon identification tags taken from each group of coupons also produced a heavy microbial growth within the boundaries of the imprint. Of particular interest was the occurrence of microbes on the beryllium coupons. Extensive work on microbial interactions with beryllium has not been reported in the relevant literature. It should be noted that none of the metal coupons had a noticeable biocidal effect on the native microbial population.

Table 15. Microbial types isolated from imprints and swabbing the surface of coupons cultured on solid media.

Samples	Media / Sample	Results
CA01-1-1	NAG imprint	Heavy growth of bacteria, fungi, actinomycetes within margin of imprint.
CA01-1-2	NAG swab	Heavy growth of bacteria, fungi, actinomycetes.
CA01-1-3	PRG swab	Acid indicated near some microbial colonies.
Teflon		
CA01-6-1	NAG imprint	Heavy growth of bacteria, fungi, actinomycetes within margin of imprint.
CA01-6-2	NAG swab	Heavy growth of bacteria, fungi, actinomycetes.
CA01-6-3	PRG swab	Acid indicated near some microbial colonies.
Teflon		
CA02-1-1	NAG imprint	Heavy growth of bacteria, fungi, actinomycetes within margin of imprint.
CA02-1-2	NAG swab	Heavy growth of bacteria, fungi, actinomycetes.
CA02-1-3	PRG swab	Acid indicated near some microbial colonies.
	NAG imprint	Heavy growth of bacteria, fungi, actinomycetes within margin of imprint.
Teflon	NAG swab	Heavy growth of bacteria, fungi, actinomycetes.
	PRG swab	No acid indicated.
CA02-6-1	NAG imprint	Heavy growth of bacteria, fungi, actinomycetes within margin of imprint.
CA02-6-2	NAG swab	Heavy growth of bacteria, fungi, actinomycetes.
CA02-6-3	PRG swab	Acid indicated near some microbial colonies.
Teflon		
CA02-3-1	NAG imprint	Heavy growth of bacteria, fungi, actinomycetes within margin of imprint.
CA02-3-2	NAG swab	Heavy growth of bacteria, fungi, actinomycetes.
CA02-3-3	PRG swab	Acid indicated near some microbial colonies.
CA02-3-4		
CA02-3-5		
CA02-3-6		
CA02-3-7		
CA02-3-8		
Teflon		
CA01-3-8	NAG imprint	Heavy growth of bacteria, fungi, actinomycetes within margin of imprint.
CA01-4-7	NAG swab	Heavy growth of bacteria, fungi, actinomycetes.
CA01-4-6	PRG swab	Acid indicated near some microbial colonies.
CA02-4-4		
CA02-4-7		
CA02-4-6		

All of the recovered coupons had at least some organisms associated with the surface that could produce organic acids, with acid production sufficient to cause a color change in the PRG agar pH indicator. This indicator was used for the detection of organic acids that change the surrounding pH to 4 or less. Analysis also showed that samples of the soil surrounding the coupons supported a diversity of

microbial species. These data indicated that the soil from all locations served as a source of microbial inoculum. In turn, the surfaces of the coupons were inoculated by the prevalent microbes.

Apparently, in most cases, the microbes were attached to the surface of the coupon, since the coupons were removed from the incased soil without noticeable adherence of soil. Coupons composed of carbon steel, aluminum, and beryllium, however, did have noticeable amounts of adhering soil. As much of this soil as possible was scraped from the surface using a sterilized spatula. Because of the adhering soil, it is possible that an undetermined amount of the recovered microbes might have been in the soil and not actually adhered to the coupon surface.

Because microbes were found on all the coupons and there is corrosion occurring on some of the metals (carbon steel, aluminum, and beryllium showed the initial effects of corrosion with areas of discoloration and surface roughness), additional analysis will have to be performed to examine coupon surfaces for biofilm development. This should include using various staining techniques, and microscopic examination of coupon surfaces with electron and light microscopy. These activities need to be budgeted into follow-on coupon recovery and examination efforts.

Results from the serum bottle analysis of the soil and coupons confirmed the presence of heterotrophic microbes, some of which were organic acid producing. These results are summarized in Table 16. There was no indication of the presence of denitrifying bacteria or the mineral acid producing *Thiobacillus thiooxidans* (*T. thio.*). Sulfate reducing bacteria (SRB) were detected in soil from the CA01-1 and CA02-1 locations but not on any of the coupons. Denitrifying microbes were not detected in any samples. The previous isolation of heterotrophic and organic acid producers on PRG agar was a confirmation of the serum bottle analysis. The absence of denitrifying microbes was an indication that the soil environment, at the time of the analysis, was not experiencing anaerobic conditions suitable for the growth of nitrate reducing microbes. Metal corrosion can be linked to those reducing environments. However, the occurrence of SRB in the two soil samples indicated that some anaerobic macro or micro environments did exist near the buried coupons. More importantly, because SRB are associated with metal corrosion, their occurrence in the soil showed that there is a source of inoculum for initiation of SRB growth in biofilm on the surface of the coupons. Soil moisture was sufficient in all samples to allow for the presence of viable microbes.

Table 16. Microbial types isolated from swabbing the surface of coupons and culturing in serum bottle media.

Sample	Metal Type	% Soil Moisture	Microbial Characteristics				
			Heterotroph	Denitrifier	Acid Prod	*T. thio.*	SRB
CA01-1-1 CA01-1-2 Teflon	CS 316L SS		+	-	+	-	-
CA01-1-3	Ferralium		+	-	-	-	-
Soil		11.6	+	-	+	-	+
CA01-6-1 CA01-6-2 CA01-6-3 Teflon Soil	316L SS Ferralium Zircaloy	12.4	+	-	+	-	-
CA02-1-1 CA02-1-2	Zircaloy Aluminum		+	-	+	-	-
CA01-1-3 Teflon	Aluminum		+	-	-	-	-
Soil		16.1	+	-	+	-	+
CA02-6-1 CA02-6-2 CA02-6-3 Teflon Soil	Zircaloy Zircaloy 316L SS	15.8	+	-	+	-	-
CA02-3-1 CA02-3-2 CA02-3-3 CA02-3-4 CA02-3-5 CA02-3-6 CA02-3-7 CA02-3-8 Soil	304L SS CS 316L SSW Ferralium 316L SSW CS Aluminum 316L SS	15.4	+	-	+	-	-
Teflon			+	-	-	-	-
CA01-3-8 CA01-4-6 CA02-4-4 CA02-4-7 CA02-4-6	Beryllium Inconel Beryllium Beryllium Inconel		+	-	+	-	-
CA01-4-7	Beryllium		+	-	-	-	-

4.4.2 Soil Gas Sampling

Classification of microbes based on their need for oxygen as an electron acceptor has produced categories that range from aerobic, to facultative aerobic, to strict anaerobic. There are physical/chemical methods, such as redox potential and actual measurement of oxygen (O_2) in the soil atmosphere. For this study, O_2 and other select soil atmospheric gases were used.

Oxygen (as an electron acceptor) concentration is important in determining the physiological type of microbes that can exist in a soil environment. The content of O_2 in the soil depends on the percent of the volume of soil pores that are filled with water. So it is expected that as the volume of water increases in a soil pore, the volume of O_2 and other soil gases (the soil atmosphere) will decrease. The soil atmosphere is replenished by the infiltration of atmospheric gases into the soil pores as they drain. Because infiltration decreases as a factor of depth in soil, gas exchange in deeper soil horizons (i.e., greater than a meter) can be limited. However, the concentration of individual gases in the soil horizon is dependent not only on soil permeability but also on the activity of the microbes present. When aerobic microbes metabolize available carbon compounds, they use O_2 as an electron acceptor and respire carbon dioxide (CO_2). Where aerobic microbes are present, it is expected that O_2 concentrations will decrease in horizons where gas exchange is limited. In addition, it is to be expected that even in well aerated soils, the concentration of CO_2 will be at a level several times above that of the atmosphere (Alexander 1961). In soil horizons with limited O_2, it is expected that other gases such as methane (CH_4) will be also be elevated above the atmospheric values. Thus, measurement of the concentration of various gases (i.e., O_2, nitrogen (N_2), CO_2, and CH_4) serves as a remote indicator of microbial activity, because these gases have a microbial linkage.

The procedures used to collect the soil atmosphere samples for this study are described in Appendix B. Results are presented in Table 17. Known gas concentrations were used to calibrate analytical procedures before the soil atmosphere samples were analyzed. Concentrations of N_2 and O_2 in the laboratory atmosphere were used as standards, while specialty calibration gases were used for CO_2 and CH_4 (because of their normally low atmospheric content). As can be seen from the data, (Table 17) comparisons of the concentrations of N_2 and O_2 in the laboratory atmosphere fit very well with that of clean dry air at sea level (an average of 79.39 ± 0.02 vs 78.09 for N_2 and 20.61 ± 0.02 vs 20.94 for O_2). Analyzed quantities of CO_2 and CH_4 were correct for each calibration gas sample.

In general, the soil atmosphere recovered from near the coupons at the 4-ft and 10-ft depths, as shown in Table 17, corroborate the occurrence of microbial activity at depth (Table 16). The O_2 and CO_2 data were indicators of microbial activity. Note that the O_2 concentration at both soil depths was less (by ~2%) than that of the laboratory atmosphere and the standard sea level atmosphere. Also, the average O_2 content at the deepest depth (18.78 %) appeared to be less than that of the 4 ft. level (19.12 %) though these numbers are not statistically different. Most interesting, however, was that the CO_2 concentrations at both depths (0.78 % at 4 ft and 1.68 % at 10 ft) exceed the atmospheric concentration (0.03 %) by 20 to over 500 fold, respectively. These data were consistent with those of other soil atmosphere studies. Alexander (1961) showed that it was common for CO_2 concentrations to exceed the atmospheric level by at least a factor of 10 to 100, while at the same time O_2 in the soil was less plentiful than atmospheric concentrations. The difference in the composition of the above ground and below ground atmospheres arises from the respiration of microbes and plant roots—living organisms consuming O_2 and releasing CO_2. The higher CO_2 concentration at the 10-ft level was likely not the result of root activity, since connected roots were not found at this depth.

Table 17. Concentration of selected gases from the soil atmosphere.

Sample Description	Nitrogen Conc. (%vol)	Oxygen Conc. (%vol)	Carbon Dioxide (%vol)	Methane Conc. (ppmv)
4 ft	78.14	19.46	0.84	4.45
4 ft	75.90	18.89	0.79	3.00
4 ft	78.65	19.60	0.77	1.60
4 ft	75.70	18.87	0.77	2.57
4 ft	75.21	18.76	0.74	1.00
Ave. 4 ft	76.72±1.56	19.12±0.38	0.78±0.04	2.04±0.91[a]
10 ft	81.79	19.28	1.75	18.01
10 ft	78.03	18.41	1.62	2.11
10 ft	78.96	18.67	1.70	1.14
10 ft	79.47	18.78	1.67	2.58
Ave. 10 ft	79.56±1.60	18.78±0.36	1.68±0.05	1.94±0.73[a]
Atmosphere	79.39	20.61		
Atmosphere	79.41	20.59		
Atmosphere	79.37	20.63		
Ave. Atmosphere	79.39±0.02	20.61±0.02		
50 ppmv methane				50.00
0.1% CO_2			0.10	
1.0% CO_2			1.00	
10.0% CO_2			10.00	
Clean dry air sea level	78.09	20.94	0.0332	1.50

a. First determination not included in average.

Diffusion of the gases tends to balance somewhat the concentration gradient so that the content of O_2 and CO_2 is governed by both the diffusion rate and by the rate of respiration. As a rule, the O_2 content declines and the CO_2 level in the gas phase increases with depth. Changes in the soil atmosphere alter the size and functions of the microflora as both CO_2 and O_2 are necessary for growth. A soil that is sufficiently well aerated for the growth of higher plants does not necessarily contain an optimum concentration of O_2 for the microflora.

The average CH_4 concentration (discounting the initial sample) for both depths was nearly the same, at ~ 2 ppmv. This was somewhat greater than that of the sea level atmosphere, 1.50 ppmv. It is not known why the first samples taken at each level (4 ft and 10 ft) were higher in CH_4 than the subsequent

samples. This was not the case with any of the other gases. It is possible that the CH_4, being more buoyant than the other gases, tended to fill the first sample at higher concentrations.

Nitrogen was included in the analysis because not only is it the most abundant gas in the atmosphere, it is also the most abundant inert gas (biologically non reactive except for nitrogen fixation, which was not considered as a major sink in the berm soil). It provides an indication whether or not the soil was permeable enough to allow atmosphere gas transfers. From these data, it appears that atmosphere gas transfer is occurring. The N_2 concentration at both depths is within about 1% of the known atmospheric concentration.

4.4.3 Discussion of Results

Evidence of acid production by some of the microbial colonies cultured during this study, combined with the presence of acid-producing bacteria in many of the samples and the presence of SRB in a few of the samples, indicates a possibility that microbiologically-induced corrosion might be a factor at the Test Berm, and by extension, at the SDA. The results of this study represent a beginning point from which additional investigations can be launched in conjunction with future coupon recoveries and examinations. Such investigations might include:

- Examining coupon surfaces for biofilm development, including the use of various staining techniques, and microscopic examination of coupon surfaces with electron and light microscopy.
- Identifying microorganism genus and species
- Conducting bacteria counts for SRB and other microbes of interest for comparison with criteria specified in the literature
- Comparing SDA and Berm microorganism characteristics.

For example, Stein (1993) cites criteria published by Ronay et al. (1987) that specify SRB counts that correspond with MIC of varying severity, as listed in Table 18.

Table 18. General SRB criteria for MIC in soil.

Bacteria counts per gram of soil	MIC severity
10,000 or greater	Severe
5,000 to 10,000	Moderate
Less than 5,000	No MIC

5. CONCLUSIONS AND RECOMMENDATIONS

5.1 First Year Corrosion Rate Summary

The austenitic stainless steels (304L and 316L), nickel-based alloy (Inconel-718), and Zircaloy 4 had non-measurable corrosion rates for underground exposure for a one-year test period. Of the materials tested, Beryllium S200F and carbon steel had significant one-year corrosion rates. The only metals that show any effect of soil depth and corrosion rate are the beryllium and carbon steel.

These initial results reinforce the conclusion by Nagata and Banaee that the standard corrosion rates developed by Oztunali and Roles (1986) and used by Maheras et al. (1994) in the SDA performance assessment may be considerably higher than actual corrosion rates in SDA soils. Follow-on work to retrieve coupons and obtain addition data for longer corrosion times should be actively pursued to reduce uncertainties in the source term used in the SDA performance assessment.

5.2 Beryllium

The beryllium has emerged as the single most interesting material after just one year of underground exposure to corrosion conditions. This test presents the first occurrence of a controlled field study of underground corrosion effects of beryllium. Since the results are significant, a separate study on beryllium corrosion is warranted. A follow-on study for beryllium cleaning and measurement uncertainties would add credibility to the beryllium corrosion rates. Follow-on years recovery and measurements are also essential to compare differences in the two depths as well as to examine and define corrosion initiation and propagation.

The SDA has many disposed waste blocks of activated Beryllium S200F. Of particular concern is the long-lived radioactivity of the C-14 contained in the beryllium. The beryllium corrosion rate from the one-year results needs to be correlated to the buried waste beryllium. The source term from the activated Beryllium S200F should be calculated. Other aspects of beryllium corrosion, such as release and transport mechanisms, should be examined.

5.3 Soil Characteristics

To fully correlate the findings of the corrosion results at the Engineered Barriers Test Berm Extension with the SDA, additional investigations need to be done. A study should compare soil moisture content in the Berm with soil moisture content at the SDA. Additional soil resistivity measurements should be taken on the test berm at different times of the year to account for different soil moisture contents. Soil characteristics, such as pH and compositions, also need to be compared and documented further. Additional studies, as outlined in the LTCD Test Plan (Adler Flitton et al. 1997), should be pursued to include tests with added moisture to simulate the varied conditions at the SDA.

5.4 Microbiological Factors

The soil microbiology study found microorganisms on the surface of all the examined coupons. No conclusions can be made at present on the possibility of microbiologically induced corrosion on either the non-irradiated materials in the Berm or the activated metals at the SDA. Additional studies need to be performed to verify microbiological corrosion influences. Additional analysis will have to be performed to examine coupon surfaces for biofilm development upon recovery. Soil gas analyses should continue biannually at the Berm, and compared to SDA soil gas analyses.

6. REFERENCES

Adler Flitton, M.K., C.W. Bishop, R.E. Mizia, J.H. Wolfram, and P.K. Nagata, 1997, *Long Term Corrosion/Degradation Test, Test Plan*, INEEL/INT-97-00276.

Alexander, M., 1961. *Introduction to Soil Microbiology*, John Wiley and Sons, Publishers.

ASTM Method D421/422, "Laboratory Determination of Water (Moisture) Content of Soil and Rock," American Society for Testing and Materials.

ASTM Method D2216-80, "Dry Preparation of Soil Samples for Particle-Size Analysis and Determination of Soil Constants," American Society for Testing and Materials.

ASTM Method G1, "Practice for Preparing, Cleaning, and Evaluating Corrosion Test Specimens," American Society for Testing and Materials.

ASTM Method G4, "Standard Guide for Conducting Corrosion Coupon Tests in Field Applications," American Society for Testing and Materials.

ASTM Method G15, "Standard Terminology Relating to Corrosion and Corrosion Testing," American Society for Testing and Materials.

ASTM Method G16, "Standard Guide for Applying Statistics to Analysis of Corrosion Data," American Society for Testing and Materials.

ASTM Method G51, "Standard Test Method for Measuring pH of Soil for Use in Corrosion Testing," American Society for Testing and Materials.

ASTM Method G57, "Standard Test Method for Field Measurement of Soil Resistivity Using the Wenner Four-Electrode Method," American Society for Testing and Materials.

Bishop, C.W., 1998, *Soil Moisture Monitoring Results at the Radiological Waste Management Complex of the INEEL, FY 1996, FY 1995, and FY 1994*, INEEL/EXT98-00941.

Black, C.A., et al. (eds.), 1965, *Methods of Soil Analysis, Part 1,* Number 9, Series Agronomy, American Society of Agronomy, Madison, Wisconsin.

Bunnel, L.R., L.A. Doremus, and J. B. Topping, 1994, *Task E Container Corrosion Studies: Annual Report,* WHC-EP-0769, Westinghouse Hanford Company, Rev. 1.

Chaker, V., 1995, "Soils," in *Corrosion Testing and Standards, Application and Interpretation,* R. Baboian, ed., American Society for Testing and Materials.

DOE, 1999, DOE Order 435.1a, *Radioactive Waste Management*" U.S. Department of Energy, July.

DOE, 1988, DOE Order 5480.2a, *Radioactive Waste Management*, U.S. Department of Energy, September.

Durr, C.L. and Beavers, J.A., "Techniques for Assessment of Soil Corrosivity," Paper 667, *Corrosion 98, NACE International, Houston, TX.*

Escalante, E., 1987, "Corrosion Testing in Soil," Metals Handbook-Vol. 13, *Corrosion,* American Society for Metals International, Metals Park, Ohio.

Escalante, E., 1995, "Soils," *Corrosion Tests and Standards*, American Society for Testing and Materials, Philadelphia.

Franklin, D.G., 1997, "The Corrosion of Zircaloy-Clad Fuel Assemblies in a Geologic Repository Environment", presented at the *Workshop on Alternative Models and Interpretations Waste Form Degradation and Radionuclide Mobilization Expert Elicitation Panel, San Francisco, CA.* December, WAPD-T-3193, Bettis Atomic Power Laboratory, West Mifflin, Pa.

Gerhold, W.G., E. Escalante, and B.T. Sanderson, 1976, *Progress Report on the Corrosion Behavior of Selected Stainless Steels in Soil Environments,* NBSIR 76-1081, National Bureau of Standards, Washington, D.C.

Gerhold, W.G., E. Escalante, and B.T. Sanderson, 1981, *The Corrosion Behavior of Selected Stainless Steels in Soil Environments,* NBSIR 81-2228 (NBS), National Bureau of Standards, Washington, D.C.

Hillner, E., D.G. Franklin, and J.D. Smee, 1994, *The Corrosion of Zircaloy-Clad Fuel Assemblies in a Geologic Repository Environment*, WAPD-T-3173, Bettis Atomic Power Laboratory, West Mifflin, PA.

Maheras, S.J., A.S. Rood, S.0. Magnuson, M.E. Sussman, and R.N. Bhatt, 1994, *Radioactive Waste Management Complex Low-Level Waste Radiological Performance Assessment,* EGG-WM-8773, EG&G Idaho, Inc.

Nagata, P.K., and J. Banaee, 1996, *Estimation of the Underground Corrosion Rates for Low-Carbon Steels; Types 304 and 316 Stainless Steels; and Inconel 600, 601, and 718 Alloys at the Radioactive Waste Management Complex*, INEL-96/098, Lockheed Martin Idaho Technologies Company.

Oztunali, O.I., and G.W. Roles, 1986, *Update of Part 61 IMPACTS Analysis Methodology*, NUREG/CR-4370, Vols. 1 and 2.

Pfeifer, M.K., 1997, *Background Resistivity and Conductivity for the Long Term Corrosion/Degradation Test Project*, EDF-RWMC-985.

Palmer, J.D., 1974, "Soil Resistivity-Measurement and Analysis", Materials Performance, National Association of Corrosion Engineers.

Palmer, J.D., 1989, "Environmental Characteristics Controlling the Soil Corrosion of Ferrous Pipe," *Effects of Soil Characteristics on Corrosion, ASTM STP 1013,* American Society for Testing and Materials.

Piciulo, P.L., C.E. Shea, and R.E. Barietta, 1985, *Analyses of Soils from the Low-Level Radioactive Waste Disposal Site at Barnwell, SC, and Richland, WA*, NUREG/CR-4083.

Romanoff, M., 1957, *Underground Corrosion*, NBS 579, NTIS PB 168350, National Bureau of Standards.

Ronay, D., I. Fesus, and A. Wolkober, 1987, "New Aspects in Research in Biocorrosion of Underground Structures," presented at *UK Corrosion '87, Brighton, UK*.

Rood, A.S., and M.K. Adler Flitton, 1997, *Identification of Metal Alloys for Inclusion into Corrosion Test,* RWMC-EDF-931, INEL/INT-97-00038, Lockheed Martin Idaho Technologies Company.

Stein, A.A., 1993, "MIC Treatment and Prevention," in *A Practical Manual on Microbiologically Influenced Corrosion,* Gregory Dobrin, ed., NACE International, Houston, TX.

Tullis, J.A., S.T. Marts, M.C. Pfeifer, and J.B. Sisson, 1993, *Corrosive Properties of Backfill Soils at the Radioactive Waste Management Complex*, Idaho National Engineering Laboratory, EGG-GEO-10382, EG&G Idaho, Inc.

Wilkins, S.C., B.C. Norby, and E.C. Hales, 1998, *Test Results, Weight Loss Measurements in Coupon Control blank Cleaning for the Long-Term Corrosion/Degradation Test*, INEEL-INT-97-01196, EDF-RWMC-994.